SEG Special Publications, no. 23, pp. 203–226

Chapter 10

Olympiada Gold Deposit, Yenisei Ridge, Russia

A. M. Sazonov,[1] K. V. Lobanov,[1,2] E. A. Zvyagina,[1] S. I. Leontiev,[1] S. A. Silyanov,[1] N. A. Nekrasova,[1] A. Y. Nekrasov,[3] A. B. Borodushkin,[3] V. A. Poperekov,[3] V. V. Zhuravlev,[3] S. S. Ilyin,[3] Yu.A. Kalinin,[4] A. A. Savichev,[5] and A. S. Yakubchuk[6,7,†]

[1]*Siberian Federal University, 79 Svobodnyi Prospect, Krasnoyarsk 660041 Russian Federation*

[2]*Orsu Metals Corporation, Unit 1–15782 Marine Drive, White Rock, British Columbia, Canada V4B 1E6*

[3]*PJSC Polyus, 24 Krasnoi Gvardii Street, Krasnoyarsk 660000 Russian Federation*

[4]*Institute of Geology and Mineralogy SB RAS, 3 Akademika Koptyuga Street, Novosibirsk 630090 Russian Federation*

[5]*Saint-Petersburg Mining University, 2, 21st Line, St. Petersburg 199106, Russian Federation*

OOO Norilskgeologia, 11 Grazhdanskiy Prospekt, St. Petersburg 195220, Russian Federation

[6]*Geological Institute, Russian Academy of Sciences, 7 Pyzhevskiy Pereulok, Moscow 119017 Russian Federation*

[7]*Orsu Metals Corporation, Unit 1–15782 Marine Drive, White Rock, British Columbia, Canada V4B 1E6*

Abstract

The Olympiada deposit, containing >1,560 metric tons (t; 50 Moz) of gold at an average grade of 4 to 4.6 g/t Au, occurs in central Siberia, Russia. Over 30 years, the deposit produced more than 580 t of gold, including 200 t from oxidized ore grading 11.1 g/t. The deposit forms a 2-km-long, steeply dipping system, which is traced downdip for 1.7 km. It occurs in the Neoproterozoic orogen of the Yenisei Ridge at the western margin of the Siberian craton. This and other gold deposits in the district are controlled by the large, long-lived Tatarka-Ishimbino tectonic zone, marking a suture between terranes chiefly consisting of deformed Meso- to Neoproterozoic carbonate-clastic sedimentary rocks. The combination of lithologic and structural factors was critical for localization of gold mineralization associated with calcic and siliceous alteration accompanied by early arsenic and late antimony sulfides. As a result, very fine (10 μm) and high fineness (910–997) gold associates with diverse sulfides, especially arsenopyrite, and commonly contains mercury, similar to some characteristics of Carlin-type deposits.

Geochronologic studies suggest that mineralization was formed during several stages between 817 and 660 Ma. The isotopic composition of Os and He, along with presence of anomalous Ni, Co, and Pt, points to a mantle mafic source, whereas isotopic composition of Pb and S suggest a contaminated crustal source, i.e., originating from a mix of mantle and crustal fluids.

Introduction

The Olympiada Au deposit was the largest gold producer in Russia for many decades. It is situated 430 km north from the city of Krasnoyarsk and 55 km south from the city of Severo-Yeniseisk in the taiga mountainous area in the 650- to 1,100-m-high Yenisei Ridge (Fig. 1A).

The Olympiada deposit is mined by Polyus Gold, which also operates several nearby deposits (Blagodatnoe, Poputninskoe, Titimukhta, Panimba). In 2017, Polyus Gold produced from this cluster nearly 20.6 million metric tons (Mt) of ore, containing 63.6 t Au (Fig. 1B). At Olympiada, the company extracted 12.3 Mt of ore, grading 3.8 g/t Au, and produced 36.4 t Au from the Eastern (main) and Western (subordinate) open pits. The depth of the Eastern pit reached 550 m in 2018, and the company is potentially considering an underground operation. During the initial years, only oxide ores were processed, whereas sulfide ores were stockpiled. Polyus Gold developed a proprietary biooxidation technology, BIONORD, for treatment of refractory sulfides. Since 2007, sulfide ores, processed at three plants, have been a principal source of gold (Sovmen et al., 2009).

†Corresponding author: e-mail, slaurum@aol.com

Exploration History

Exploration on the Yenisei Ridge started some 180 years ago after discovery of placer gold deposits. Since then, the placers produced some 900 t of gold, and >880 t of gold were also extracted from hard rock. Placer production reached its peak in the mid-20th century, whereas large-scale hard-rock gold production started only in the 1990s. Mkrtychyan (2007) estimated that the Yenisei gold province may potentially host up to 7,500 t of gold.

Placer gold was discovered near the future Olympiada deposit in the Innokentievskiy (1854) and Olympiadinskiy (1885) Creeks. In the mid-20th century, geologists discovered an antimony occurrence, which was named Olympiada (1944), followed by discovery of satellite tungsten (Olenie in 1954 and Vysokoe in 1955) and mercury (Pravoberezhnoe in 1972) mineralization. Although crushing of grab samples from these occurrences revealed the presence of gold grains, this fact did not attract much attention. In 1964, geologists of the Krasnoyarsk Geological Administration discovered hydrothermally altered rocks with disseminated sulfides at the drainage divide between the Olympiadinskiy and Innokentievskiy Creeks. Hand samples revealed up to 10 to 20 g/t Au. In 1968 to 1974, Kruglov and Li, who worked for the Krasnoyarsk

doi: 10.5382/SP.23.10; 24 p.

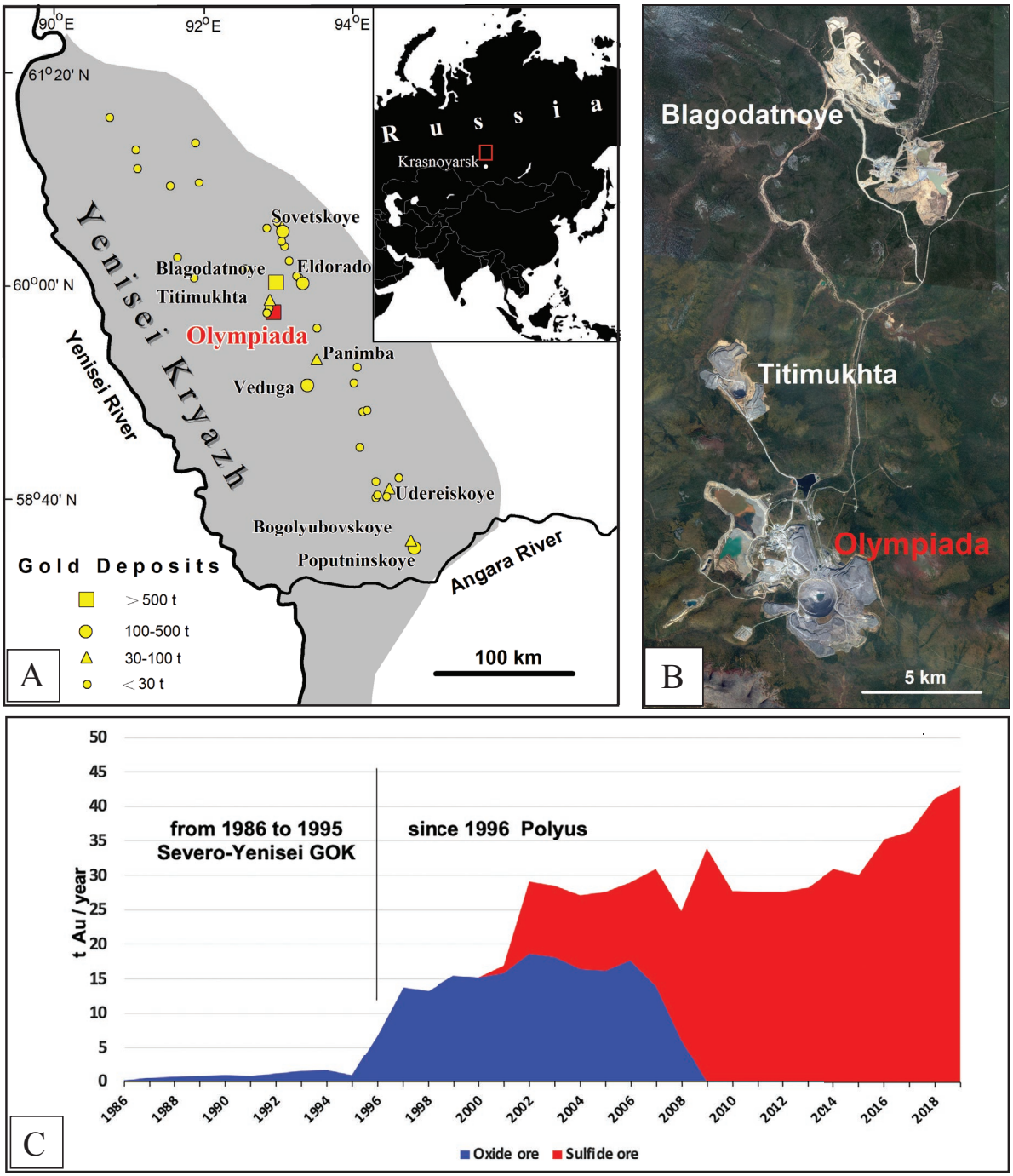

Fig. 1. A. Location of principal gold deposits in the Yenisei Ridge (Kryazh). B. Mining cluster of Polyus Gold. C. Gold production from the Olympiada deposit according to Polyus Gold. Between 1986 and 2017, 587 t of gold was recovered. The 2018 reserves stood at 938 t Au.

Branch of the Siberian Research Institute for Geology, resampled Olympiada drill core from earlier exploration for antimony. They confirmed gold mineralization in altered rocks and identified disseminated gold-sulfide-type mineralization, in contrast to previously discovered and mined gold-bearing quartz vein deposits at the Yenisei Ridge.

In 1975 to 1977, follow-up exploration by Severnaya Expedition of KrasnoyarskGeologia in the Verkhnee Enashimo cluster discovered the Olympiada gold deposit. In 1978 to 1980, work continued mostly at the Western area, containing (as became evident later) only 15% of total gold endowment. In 1980 to 1984, the first drill holes during detailed exploration of the Eastern area intercepted abundant and gold-rich oxide as well as sulfide mineralization to a depth of 700 m. This dramatically reclassified Olympiada as a large deposit. In 1985, oxide reserves ($B+C_1$ in Russian classification) were

estimated at 14 Mt, grading 10.7 g/t Au, totaling 150.7 t Au and justifying the beginning of modest mining of oxide ores (Fig. 1C) from the Eastern and then the Western pits. By 2007, Polyus completed mining of the oxide material, extracting 17.3 Mt, grading 11.1 g/t Au for 193.3 t gold.

In 1990 to 1992, exploration also included additional drilling and metallurgical studies of sulfides, as well as hydrogeologic and other technical studies. The 1993 B + C_1 + C_2 reserves contained 542 t Au, of which sulfide ores comprised 102.5 Mt, grading 3.78 g/t Au, supplemented by by-product silver and antimony reserves. The latter can be extracted into a flotation concentrate. Sulfide ores were initially stockpiled without processing. By 2000, Polyus developed biooxidation technology to extract gold from flotation concentrate, and by 2010, the company constructed two plants to process 3 and 5 Mt per annum of sulfide ore.

In 2008 to 2011, Polyus drilled deep levels of the Eastern area, as well as a target at the junction between West and East Olympiada, where the Promezhutochnyi (Transitional) zone was discovered (Fig. 2A). The mineralization from the Eastern area was traced to a depth of >1,300 m that can be potentially mined underground. In 2016, the company estimated new resources for open-pit (to –60mRL in the Eastern pit and to +430mRL for the Western pit at a cutoff grade of 0.75 g/t Au) and underground (using 3.0 g/t cutoff) operations (Fig. 2B). The gneiss-schist pit-constrained reserves increased by 95.8 Mt, grading 3.67 g/t Au for 351.5 t Au. The underground resources were estimated at 79.5 Mt, grading 5.55 g/t Au for 441.6 t Au.

Since discovery of Olympiada in 1975, about 22,000 m of trenches and 261,200 m of drilling in 634 holes have been completed. The total endowment of the deposit is 359.9 Mt containing 1,564 t Au. The two deepest holes, drilled in late 2017 to early 2018 (1,690 and 1,790 m), intercepted economic mineralization at -800mRL (Fig. 2C).

By early 2018, Polyus Gold had produced 587 t of gold since the beginning of operations. After commissioning the third sulfide plant in 2017, the Olympiada mine reached a 12.4 Mt/yr mining rate. The current estimated resources will sustain the operation for 25 years, with a strong possibility of further increase in endowment. The company is planning to start extraction of antimony, expecting to contribute 15% of Russian production.

Regional Geology and Metallogeny of the Yenisei Ridge

The Yenisei Ridge is a 200-km-wide Neoproterozoic accretionary-collisional orogen, extending for 700 km along the western margin of the Siberian craton (Fig. 3). It can be clearly defined using geologic and geophysical data as situated between the craton to the east and West Siberian basin to the west (Metelkin et al., 2007; Vernikovskiy et al., 2007, 2016; Likhanov et al., 2014).

The thickness of continental crust in the central part of the ridge is 51 km based on geophysical data, which decreases westward and eastward to 40 to 43 km. At >10-km depth, the width of the orogen decreases by half, with a mushroom-like shape in section view (Vernikovsky et al., 2006; Likhanov et al., 2014).

There are two segments in the orogen (South Yenisei and Trans-Angara), separated by the ENE-trending transcrustal Angara fault (Fig. 3), with most gold deposits occurring to the north of the fault. The northern segment consists of the East Angara, Central Angara, and Isakovka terranes, comprising mostly Meso- to Neoproterozoic rocks (Likhanov et al., 2014; Vernikovsky et al., 2016). These terranes are separated by the Ishimbino, Tatarka, Priyenisei, and Anikino regional faults, with the Tatarka-Ishimbino zone of regional faults, constraining the so-called Panimba anticlinorium, and representing a suture zone between the Central Angara and East Angara terranes (Fig. 3A, C). The majority of gold deposits occurs in the eastern portion of the Central Angara terrane.

The metamorphosed Precambrian sedimentary rocks dominate the Trans-Angara segment. Gneiss and schist (Teya Group) are considered the oldest stratigraphic unit. It is overlain by 14- to 17-km-thick Meso- to Neoproterozoic cyclical sedimentary sequences divided into Sukhoi Pit, Tungusik, Oslyan, Chingasan, and Taseevo Groups (Fig. 4A; Nozhkin et al., 2011). Most gold deposits occur in the lower part of the Sukhoi Pit Group, represented by clastic, carbonaceous, and calcareous clastic rocks of the Korda, Gorbilok, and Uderei Formations. Sazonov et al. (2010) estimated that the Korda Formation hosts 73% of the discovered gold (Olympiada, Blagodatnoe, Titimukhta, Tyrada, Olenie and Panimba deposits). The Gorbilok and Uderei Formations host many gold deposits and occurrences, but only account for 7% (Eldorado, Pervenets, Udarnyi) and 20% (Sovetskoe, Veduga, Bogolyubovskoe) of the known endowment, respectively. The uppermost flysch and carbonate units (Proterozoic Pogoryui and Sosnovka Formations of the Sukhoi Pit Group, Tungusik Group and Lower Cambrian strata) host only isolated gold occurrences.

The magmatic rocks are represented by numerous ultramafic to felsic intrusions, including some alkaline varieties. Granitoids, occupying 10% of the orogen and occurring predominantly within the Central Angara terrane (Fig. 3A), are most abundant, with other intrusive rocks occupying only 0.1% of the Yenisei Ridge (Sazonov et al., 2010). The most abundant granitoids can be grouped into two types of massifs: (1) 880 to 860 Ma syncollisional granitoids of the Teya and Eruda Complexes, and (2) 760 to 720 Ma syn- to postcollisional granitoids of the Ayakhta and Glushikha Complexes (Fig. 4B; Vernikovsky and Vernikovskaya, 2006). The youngest A-type granitoids, nepheline syenite, and carbonatite belong to the 650 to 630 Ma anorogenic Tatarka Complex, with associated rare metal and rare earth mineralization. The gold deposits occur 1.5 to 18 km from intrusions, and their genetic relationships are debated (Konstantinov et al., 1999; Li, 2003; Zabiyaka et al., 2004; Serdyuk et al., 2010; Nozhkin et al., 2011).

Regional metamorphism of the Trans-Angaran sedimentary formations varies from amphibolite and epidote-amphibolite facies in the lower part of the sequence (Teya Group) to greenschist facies in the bulk of the Sukhoi Pit and Tungusik Groups (Likhanov et al., 2014; Vernikovsky et al., 2016). This regional metamorphic zonation is overprinted by contact metamorphic zones around late intrusions. Greenschist facies hosts 79% of the gold deposits, whereas amphibolite and epidote-amphibolite facies account for 11% and 10%, respectively (Zabiyaka et al., 2004). However, greenschist facies rocks contain only 27% of the discovered metal, whereas epidote-amphibolite facies host 73% of the gold (Sazonov et al., 2010), largely due to the Olympiada and Blagodatnoe deposits and their satellites.

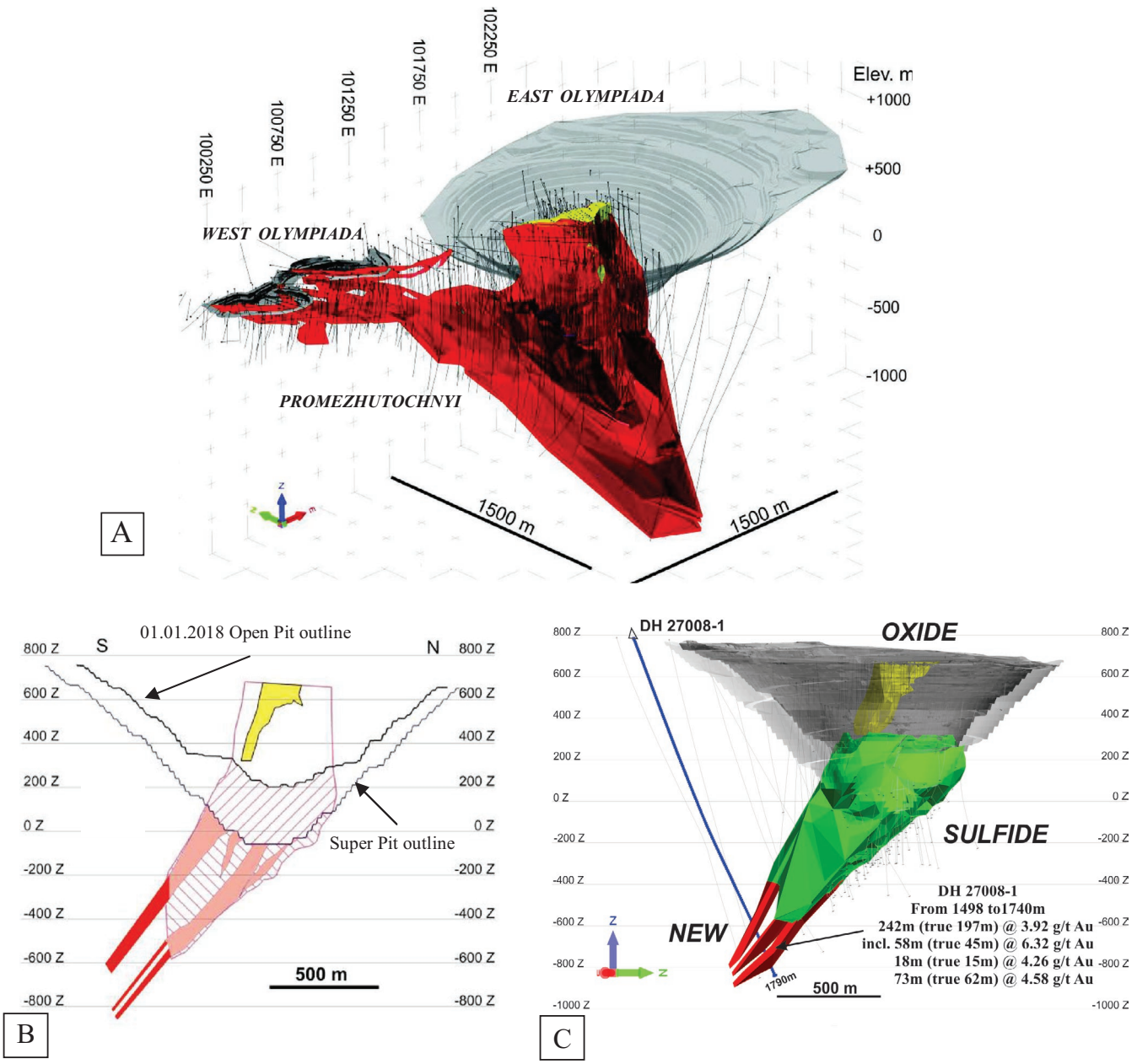

Fig. 2. Principal areas of Olympiada as of January 1, 2018. A. Pit outlines, drill hole traces, and orebodies (oxide ores in yellow, sulfide ores in red). B. Eastern lode at 0.75 g/t Au cutoff (pink contour) and at 3 g/t cutoff (solid pink, estimated in 2016). C. General view of the Eastern lode (looking west).

High-strain metamorphic zones near faults control localization of gold deposits as traced by anomalous gold against the background of country rocks. The lengths of such zones are up to 50 km but their widths rarely exceed 1.5 km. They represent the main control of the gold deposits of the Yenisei Ridge (Sazonov, 1998), where deposit types include quartz veins and veinlet systems with low sulfide and coarse gold (Sovetskoye, Eldorado, Vasilievskoye), as well as disseminated sulfides with fine gold in quartz-sericite alteration (Olympiada, Veduga, Poputninskoye, Bogolyubovskoye). Arsenic is present in all deposit types and some deposits also host economic antimony mineralization (Udereiskoye, Olympiada, Veduga). In addition to gold the Tatarka-Ishimbino fault zone hosts uranium, gold-uranium, and rare metal (Nb, Ta, REE) mineralization.

Verkhnee Enashimo Mineral District

The Olympiada gold deposit is part of the Verkhnee Enashimo mineral district (Fig. 4B, C) in the eastern portion of the Central Angara terrane. The cluster is controlled by the Ishimbino fault in the east and Tatarka fault in the west. Both are deep-penetrating fault zones, linked by closely spaced NW-trending faults, clearly visible in gravity data (Fig. 3B). The Olympiada deposit occurs closer to the Tatarka fault, whereas most other deposits are controlled by the Ishimbino fault.

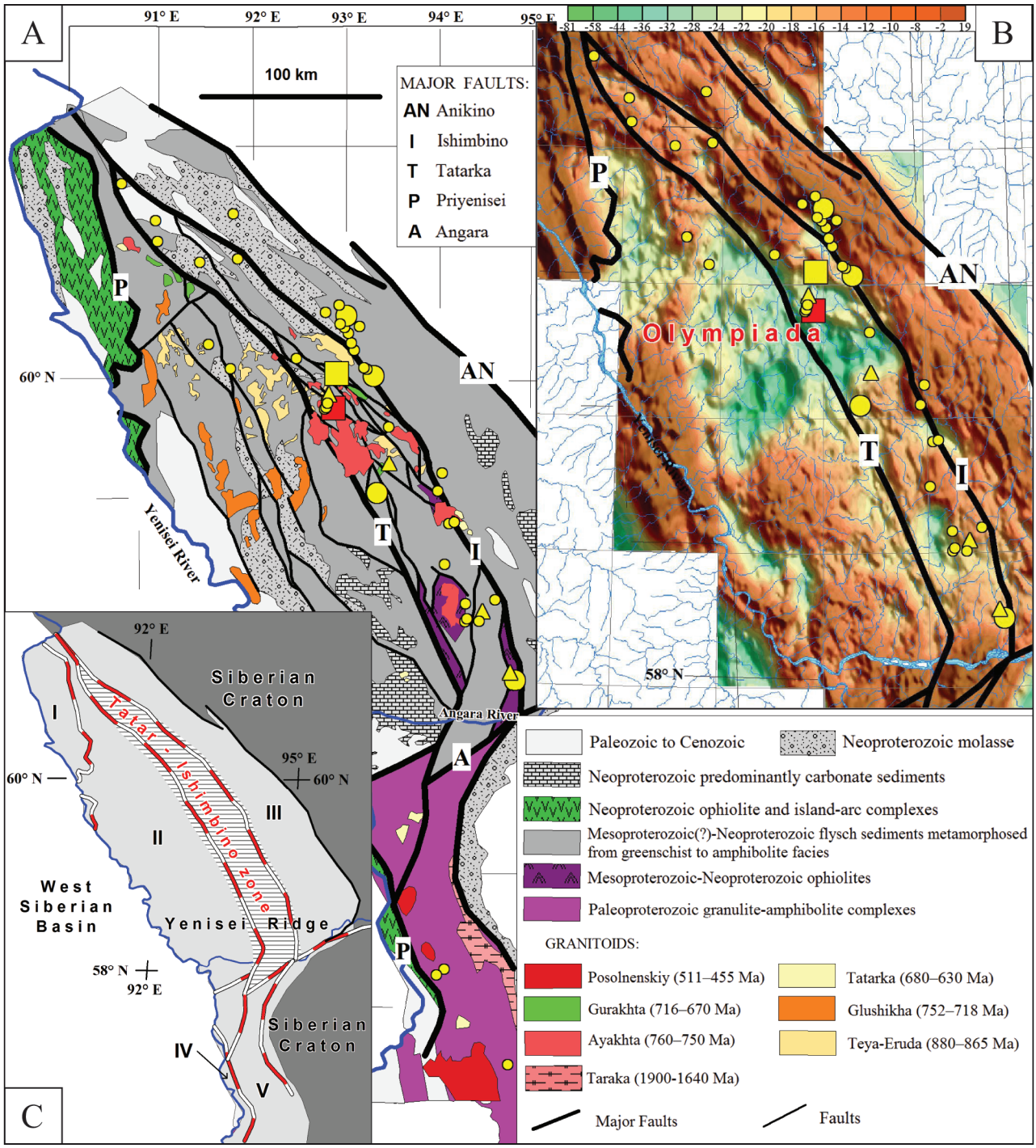

Fig. 3. Gold deposits in the Yenisei Ridge. A. Schematic geologic map (Vernikovskaya et al., 2007; Likhanov et al., 2014; Vernikovsky et al., 2016). B. Gravity map of the Trans-Angara segment (in mGal), with gravity lows corresponding to granitoid massifs. C. Terranes (I = Isakovka, II = Central Angara, III = East Angara, IV = Predivinsk, V = Angara-Kan and sutures in between). See Figure 1 for deposit symbols.

Sedimentary units

The sedimentary units occupy 70% of the Verkhnee Enashimo area. They differ in age, composition, metamorphic grade, and hydrothermal alteration type. The stratigraphic units are part of multistage thrust sheets, accompanied by widespread overturned bedding and recumbent to isoclinal folds, transected by zones of steeply dipping schistosity, mylonitic fabric, and brecciation. The crosscutting faults, revealing subvertical displacements for hundreds of meters, were reactivated several times.

The metamorphosed sedimentary succession can be divided into three units separated by angular unconformities (Fig. 4A). The onset of sedimentation is cautiously estimated

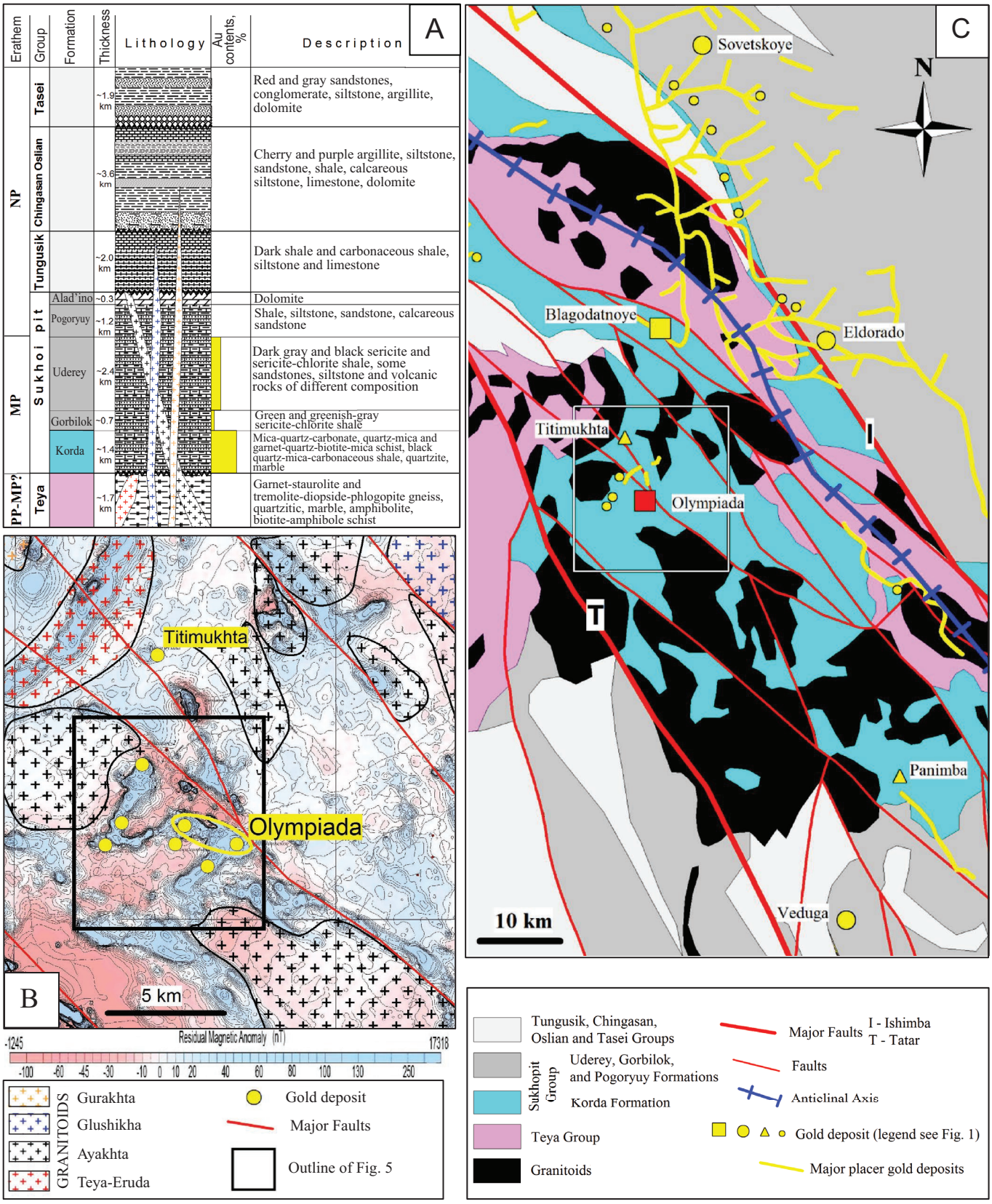

Fig. 4. Lithostratigraphic column of the Verkhnee Enashimo mineral district (A) (NP = Neoproterozoic, MP = Mesoproterozoic, PP = Paleoproterozoic); TMI aeromagnetic (B), and simplified geologic (C) maps of the Verkhnee Enashimo mineral cluster. Most gold-bearing quartz deposits, which produce placers, occur in the upper part of the Sukhoi Pit Group (Uderei and Gorbilok Formations).

as between 880 Ma (e.g., older than intruding granitoids; Vernikovsky et al., 2016) and 2600 Ma, based on Sm-Nd data on metapelites (Nozhkin et al., 2008).

Teya Group: The lower unit is exposed in the core of the NW-trending Panimba anticlinorium (Fig. 4B). Its lower part consists of high-alumina kyanite-staurolite-garnet and biotite-sillimanite gneisses, which grade upward into intercalating biotite-amphibolite schist, quartzite, amphibolite, and marble.

Sukhoi Pit Group: The middle unit consists of metamorphosed sandstone with layers of polymict conglomerate and gritstone, siltstone, and green to dark gray and black phyllite, overlain by a clastic-carbonate unit. These formations are interpreted to have been deposited at a passive margin. The lower part of this complex is metamorphosed to amphibolite and epidote-amphibolite facies (which is more typical for the Teya Group), whereas the Sukhoi Pit Group is at greenschist facies (Likhanov and Reverdatto, 2014; Vernikovsky et al., 2016).

Tungusik, Chigasan and Oslyan Groups: The upper unit consists of nonmetamorphosed Neoproterozoic to Lower Cambrian clastic and clastic-carbonate rocks (Fig. 4A) of the Tungusik, Chigasan and Oslyan Groups and their equivalents.

The lower 4.5-km part of the 6-km-thick Sukhoi Pit Group is the principal host for the gold deposits (Fig. 4A). The group reveals a well-developed transgressive-regressive cycle. Its age is constrained as Mesoproterozoic to early Neoproterozoic by U-Pb dating of detrital zircons (1345, 1205, 1125, and 1110 Ma) and paleontological data (microphytoliths and microfossils) from its upper part. The group was divided into the Korda, Gorbilok, Uderei, Pogoryui, and Alad'ino Formations (Fig. 4A).

The Korda Formation is the host for the Olympiada deposit (Fig. 5A). It consists of a 1,200- to 1,500-m-thick clastic sedimentary sequence, metamorphosed to biotite greenschist subfacies. The Korda Formation represents the transgressive part of the group. Its lower member consists of arkose metasandstone with metagritstone, which marks the unconformity with the Teya Group. This part of the formation also comprises schist, locally with garnet, and quartzite with lenses of calcareous siltstone and dolomite.

The 500- to 600-m-thick middle part of the Korda Formation hosts most gold deposits of the Olympiada cluster (Fig. 5B). It has two sulfide-rich lithologic horizons, clearly visible near Olympiada as magnetic highs (Fig. 4B) due to the presence of pyrrhotite. The lower horizon consists of mica-quartz-carbonate schist with lenses of marbleized rock. Its thickness varies between 320 and 415 m. The upper horizon consists of dark gray to black quartz-mica-carbonaceous shale with quartzitic and quartz-mica schists. Its thickness is up to 100 to 120 m. Each horizon is lithologically inhomogeneous, with gradational boundaries due to the effects of hydrothermal alteration and presence of sedimentary rocks with variable clast sizes.

The upper part of the Korda Formation consists of high-alumina garnet-quartz-biotite-muscovite schist with the characteristic presence of albite and significant abundance of chlorite.

Intrusive complexes

Teya-Eruda Complex: Granitoid intrusions occupy one-third of the deposit area (Fig. 4C), suggesting a largely leucocratic basement (Li, 2003). Granitoids of the Teya-Eruda Complex, the oldest in the Trans-Angara part of the Yenisei Ridge, formed between 880 and 865 Ma from a mixed crustal source of Paleoproterozoic age (Vernikovsky and Vernikovskaya, 2006; Likhanov et al., 2014). They mostly occur in the northern and northwestern parts of the area within the Teya Group. The intrusions are often deformed together with host metamorphic rocks (Vernikovsky et al., 2016). These massifs consist predominantly of amphibole-biotite and biotite granites, as well as granodiorite, diorite, and plagiogranite of the calc-alkaline and calcic series, plotting between S- and I-types. Concentrations of Ta, Nb, Hf, Y, Yb, Ce, K_2O, Rb, Ba, and Th are similar to both island-arc and collisional granites.

Ayakhta (Tatarka-Ayakhta) Complex: The syncollisional granitoids of the 760 to 750 Ma Ayakhta (Tatarka-Ayakhta) Complex are the most abundant (Vernikovsky and Vernikovskaya, 2006). The Chirimba massif to the south of the Olympiada cluster (Fig. 5B) is the largest intrusion (530 km^2), accompanied by smaller massifs (Tyrada, Verkhnee Enashimo). The gravity data suggest that all of them are parts of a single batholith (Fig. 3B). All massifs are similar in composition, corresponding geochemically to A-type and mixed S- and I-type granites. These granites reveal high concentrations of Rb, Ba, Th, Nb, Ce, Hf, Zr, Sm, Y, and Yb, corresponding to hybrid mantle-crustal granites. The massifs mostly consist of granodiorite (phase 1) and coarse-grained porphyritic biotite and amphibole-biotite granite of normal alkalinity (main phase 2). These massifs contain numerous internal small stocks, dikes, leucogranite veins, fine-grained granite, and aplite (phase 3).

Glushikha Complex: The much less widespread 752 to 718 Ma Glushikha Complex (Vernikovsky and Vernikovskaya, 2006) consists of predominantly coarse-grained calc-alkaline leucogranite, which is of A-type and peraluminous rare metal geochemical type, enriched in SiO_2, K, Fe, and F and depleted in Eu, Ba, and Sr.

Gurakhta Complex: The 716 to 670 Ma Gurakhta Complex (Zuev et al., 2009) is represented by a relatively large (15 × 5 km) intrusion of K-Na subalkaline biotite and amphibole-biotite granite in the axial part of the Panimba anticlinorium (Fig. 3A). Its petrogenetic and rare element composition suggest an affinity to A-type intraplate anorogenic granites.

Zakhrebetinskiy Complex: The 710 to 690 Ma Zakhrebetinskiy Complex (not shown in Fig. 3A due to its small size) is represented by small (1- to 2-m-thick and 10- to 20-m to, uncommonly, 300-m-long) dikes of trachydolerite and alkaline and nepheline syenite porphyry, forming the 20- to 30-km-long, NW-trending Enashimo swarm (Serdyuk et al., 2010; Nozhkin et al., 2011).

Olympiada mineral cluster

The Olympiada mineral cluster is controlled in the northeast and southwest by major NW-trending faults (Fig. 5A, B), interpreted as steep-dipping strike-slip faults. The cluster is bounded to the southeast and northwest by the Chirimba and Tyrada granite massifs (Fig. 5B). It is inferred that the mineral cluster sits above a large batholith, represented at surface by the two massifs and their satellites (Li, 2003; Zabiyaka et al., 2004; Serdyuk et al., 2010).

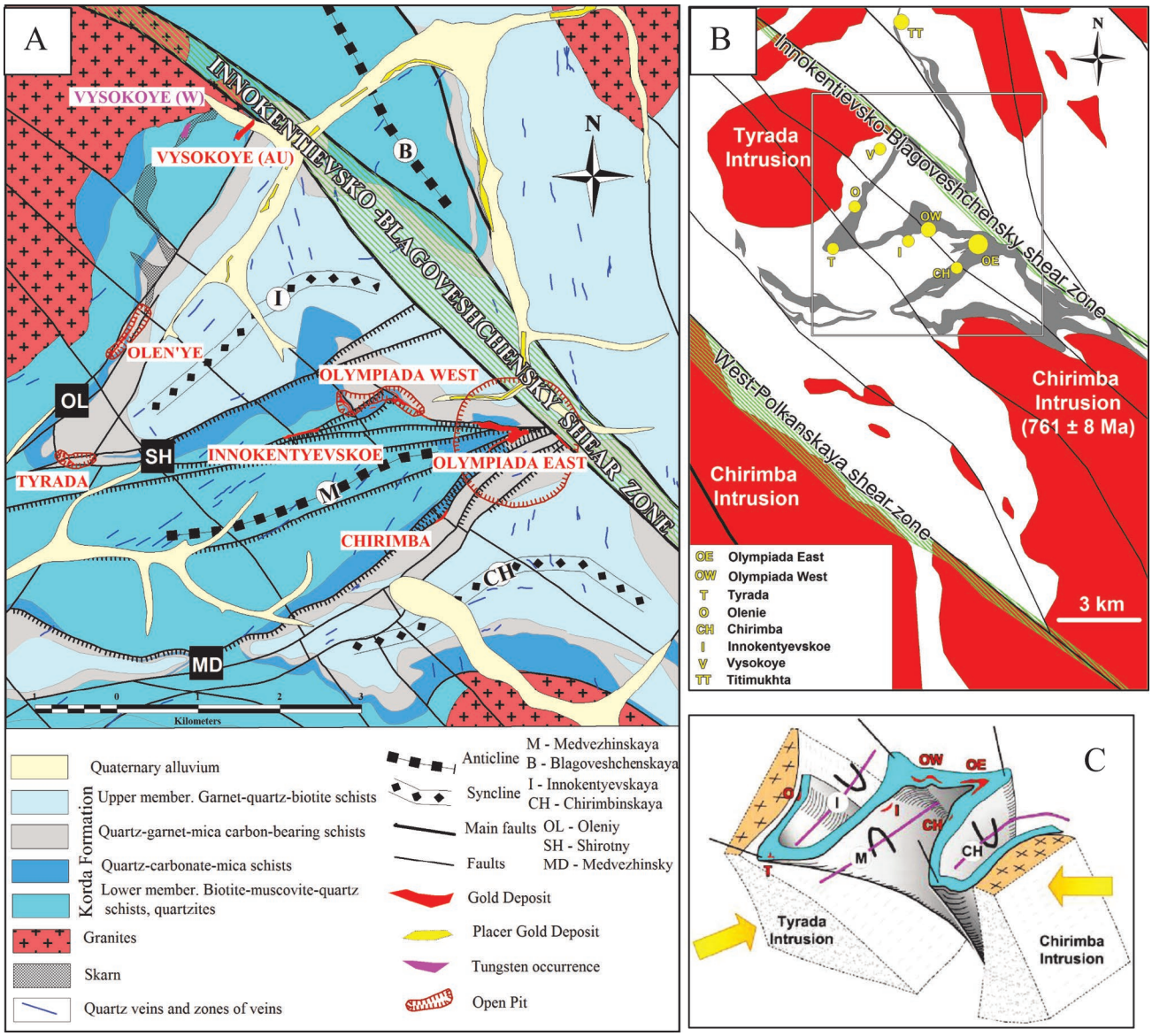

Fig. 5. Schematic geologic map (A) and principal deposits relative to the host lithologic unit (gray color), intrusions, and main faults of the Tatarka regional fault system (B), modeled to control the drag folds between the granitoid intrusions (C).

There are three main 4- to 5-km-long and 1- to 2-km-wide folds in the Olympiada cluster. Their axial planes strike east-northeast with fold hinges plunging to the east-southeast at 25° to 30° to 50° to 80° (Li, 2003; Zabiyaka et al., 2004). The three folds define a W-shaped pattern in plan view, clearly seen in the magnetic map (Fig. 4B) and represented schematically in Figure 5C.

Medvezhinskaya anticline: The Medvezhinskaya anticline is a principal host of gold mineralization in the cluster. This N-verging anticline plunges at 50° to 80° to the east-southeast, and its limbs dip 30° to 50° SE, with steeper dips in the northern limb. The northern limb has an S-shaped kink in the area west of Olympiada (Fig. 6). At surface, the limbs of the fold are defined by the ore-hosting quartz-garnet-mica-carbonaceous shale and quartz-carbonate-mica schist, with lenses of marmorized limestone; its core exposes the underlying biotite-muscovite-quartz schist (Fig. 5A). Most of the Olympiada gold endowment is localized within the closure area of the anticline (East Olympiada), with a much smaller endowment along the limbs.

Northwest- and NE-trending faults, mainly steep normal and strike-slip faults, offset the lithologic markers. In addition, there are numerous strata-bound schistose zones, meters to hundreds of meters thick, occurring along the boundaries of lithologically contrasting layers, some containing gold mineralization.

Innokentievsko-Blagoveshchenskaya shear zone: The largest fault zones in the cluster are Innokentievsko-Blagoveshchenskaya, Shirotnaya, and Olenia (Fig. 5A). The Innokentievsko-Blagoveshchenskaya shear zone is a strike-slip fault, truncating the Olympiada deposit in the northeast and a set of ENE-trending faults. It consists of a 600-m-wide corridor of sheared rocks with a clear NW-striking, subhorizontal lineation.

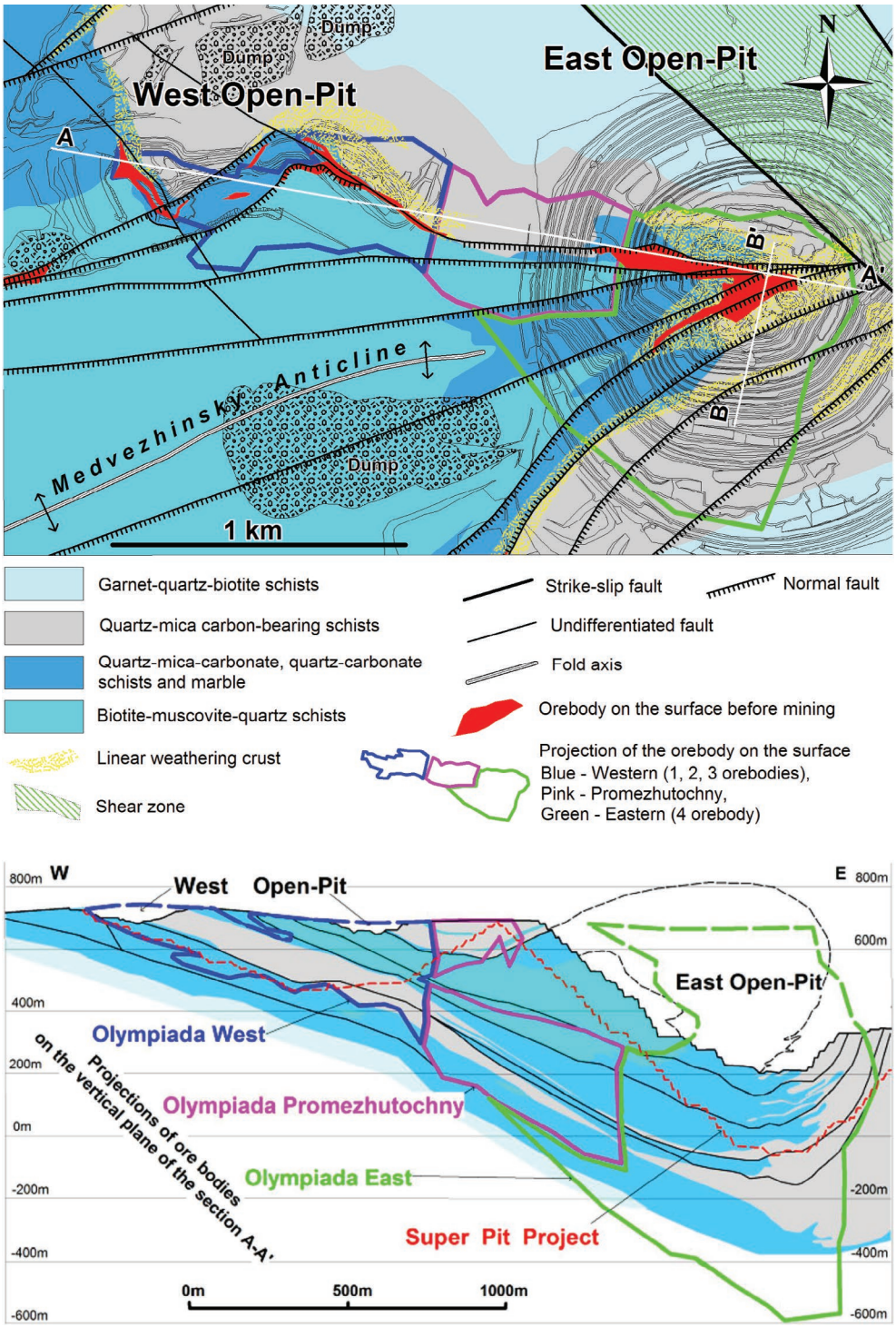

Fig. 6. Geologic map and west-east section (A-A') relative to the 2018 pits at the Olympiada deposit. See Figure 7 for the cross section along line B-B'.

Medvezhinskaya shear zone: The Medvezhinskaya shear zone strikes along the southeastern limb of the anticline, controlling East Olympiada in the south. The fault dips steeply (60°–80°) to the south-southeast (Fig. 5A) and is interpreted as a normal fault with displacements of 10 to 100 m. It is marked by a zone of intense fracturing, schistosity, and brecciation, commonly hydrothermally altered and host to gold mineralization. It is part of a set of parallel faults (e.g., Shirotnyi and Olenia; Fig. 5A) that increase in individual widths to the northeast, reaching maxima at the junction with the Shirotnaya zone.

Shirotnaya zone: The Shirotnaya zone extends from the west to the east through the entire mineral cluster. It has a complex movement history that includes normal (170 m offset) and sinistral strike-slip (230 m apparent offset). The Shirotnaya

zone controls the Tyrada and Innokentievskoe deposits as well as the northern part of East Olympiada (Fig. 5A).

Olenia zone: The Olenia zone coincides with the northwestern limb of the Innokentievskaya syncline, controlling the ore-hosting lithologic unit in the northwest. At the Tyrada and Olenie deposits, it dips 40° to 60° SE and is defined by intensely sheared and finely folded hydrothermally altered rocks.

Figure 5B shows the spatial and geometric relationships between regional faults and folds, suggesting that the Olympiada cluster occurs within a compressional duplex, formed as a result of inverse sinistral and dextral shearing between the Innokentievsko-Blagoveshchenskaya and Zapadno-Polkanskiy shear zones and recording northwest-southeast shortening along the corridor. Figure 5B shows that the internal architecture of the mineral cluster is defined by development of ENE-striking thrusts in relationship to the bounding NW-trending shear zones.

The Olympiada cluster hosts both bedrock and placer gold deposits as well as iron, polymetallic, tungsten, and lithium occurrences (Serdyuk et al., 2010). The main distinguishing feature of the cluster is the coexistence of disseminated auriferous sulfides with antimony and tungsten as well as gold and bismuth (Titimukhta), in contrast to the other deposits of the Yenisei Ridge, where gold-bearing quartz vein-type mineralization is dominant. In addition to Olympiada, disseminated gold-sulfide mineralization is known at the Tyrada, Olenie, and Vysokoe deposits as well as in the Innokentievskoe and Chirimba occurrences (Table 1), which are geologically, morphologically, and compositionally similar. More than 97% of bedrock gold endowment in the cluster resides in the Olympiada deposit.

Olympiada Gold Deposit

Geology

The economic concentrations of gold occur along the limbs and closure of the Medvezhinskaya anticline (Fig. 6). Their relative sizes are believed to be a function of their position within the anticline. At the surface, the deposit consists of the West and East Olympiada zones but drilling revealed that they merge at depth in the Promezhutochnyi zone, forming a single west-east elongated system (Fig. 6). It strikes for 2 km and extends vertically for 1.4 km (~1.7 km downdip).

West Olympiada: The West Olympiada zone includes three economic orebodies within a parasitic S-shaped fold on the northern limb of the anticline (Fig. 6). Axial planes of these folds are subvertical, dipping south or north, with hinge lines plunging 10° to 20° east. The limbs of the folds and flexures in the quartz-mica carbonate or carbonaceous horizons contain strata-bound detachments, replaced with disseminated gold-sulfide mineralization and hydrothermal alteration. This mineralization is mostly localized in carbonate rocks and to a lesser extent in the carbonaceous rocks, forming a single, continuous, strata-bound lode. In cross-section view, the lode follows the S-shaped configuration of the fold. In long section, the lode splits into several saddle-shaped branches plunging to the east (Fig. 6). The outcropping mineralization is oxidized to a depth of 60 to 200 m downdip. The distribution of gold within the orebodies is very homogeneous, with higher grades in their central parts. The average gold grade is 2.5 to 8.6 g/t Au in hypogene mineralization and 3.1 to 8.9 g/t Au in oxidized ore.

Promezhutochnyi: The Promezhutochnyi zone forms the downplunge continuation of West Olympiada to the east (Fig. 6). It forms a thick, blind orebody which merges with East Olympiada, varying in thickness from 18 to 40 m in the south to 53 to 55 m in the north, extending downplunge for 740 m, and grading 2.7 to 3.0 g/t Au. Above and below this zone are thin subparallel lens-shaped mineral zones, which pinch to the west and east. Two additional orebodies were intercepted in trenches and drill holes. They have a relatively simple tabular morphology near the folded contact between carbonate and carbonaceous rocks. One orebody is 5 to 22.5 m thick, extending for 393 m vertically and ~330 to 337 m downplunge at an average grade of 3.7 g/t Au, depending on the cutoff grades. The other orebody is 3 to 20 m thick, extending 67 to 452 m vertically and >700 m downplunge, at an average grade of 2.3 to 2.8 g/t Au.

East Olympiada: The East Olympiada zone forms the main part of the deposit, containing 90% of the gold endowment,

Table 1. Gold Deposits and Occurrences of the Olympiada Mineral Cluster and Adjacent Areas

			Mineralization		Geochemical type				
Deposit	Type	Host rock	Main	Minor	Main	By-product	Ore (Mt)	Au (g/t)	Au (t)
Olympiada	Au-As-sulf	Quartz-mica-carbonate-carbonaceous schist	pyr ar ant	py gn sf chp sch	Au	Sb	359.9	4.35	1564
Tyrada	Au-As-sulf	Quartz-mica-carbonate-carbonaceous schist	pyr ar ant	ber chp	Au	Sb	2.1	5.8	12.1
Olenie	Au-W-sulf	Quartz-mica-carbonate-carbonaceous schist	au pyr ar sch	py gn sf chp ant	Au W As	Sb	1.3	6.5	8.7
Innokentievskoe	Au-As-sulf	Quartz-mica schist	pyr ar	py gn sf chp ant	Au As	Sb	0.39	3.1	1.2
Chirimba	Au-As-sulf	Quartz-mica-carbonate-carbonaceous schist	py pyr	ar ant	Au As	W Sb	0.1	4.4	0.4
Vysokoe	Au-sulf	Quartz-mica-carbonate-carbonaceous schist	pyr ar	ant py	Au As	Sb	2	4.6	9.3
Titimukhta	Au-Bi-quartz	Hornfelsed quartz-chlorite-mica schist	au bi pyr py	hed mo	Au	Bi	25.4	3.02	76.7

Minerals: ant = stibnite, ar = arsenopyrite, au = gold, ber = berthierite, bi = bismuthine, chp = chalcopyrite, gn = galena, hed = hedleyite, mo = molybdenite, py = pyrite, pyr = pyrrhotite, sch = scheelite, sf = sphalerite, sulf = sulfide

and is still open downplunge. In early 2018, drill hole DH-27008-1 intercepted the deepest known part of the lode at 1,350 to 1,550 m below surface (Fig. 2B). Because of the near-isoclinal nature of the host anticline (Fig. 6), the thickness of the orebody doubles in the fold closure area due to the close proximity of the limbs (Fig. 7a). There are syn-folding, strata-bound faults along the lithologic boundaries, which are important for localization of mineralization.

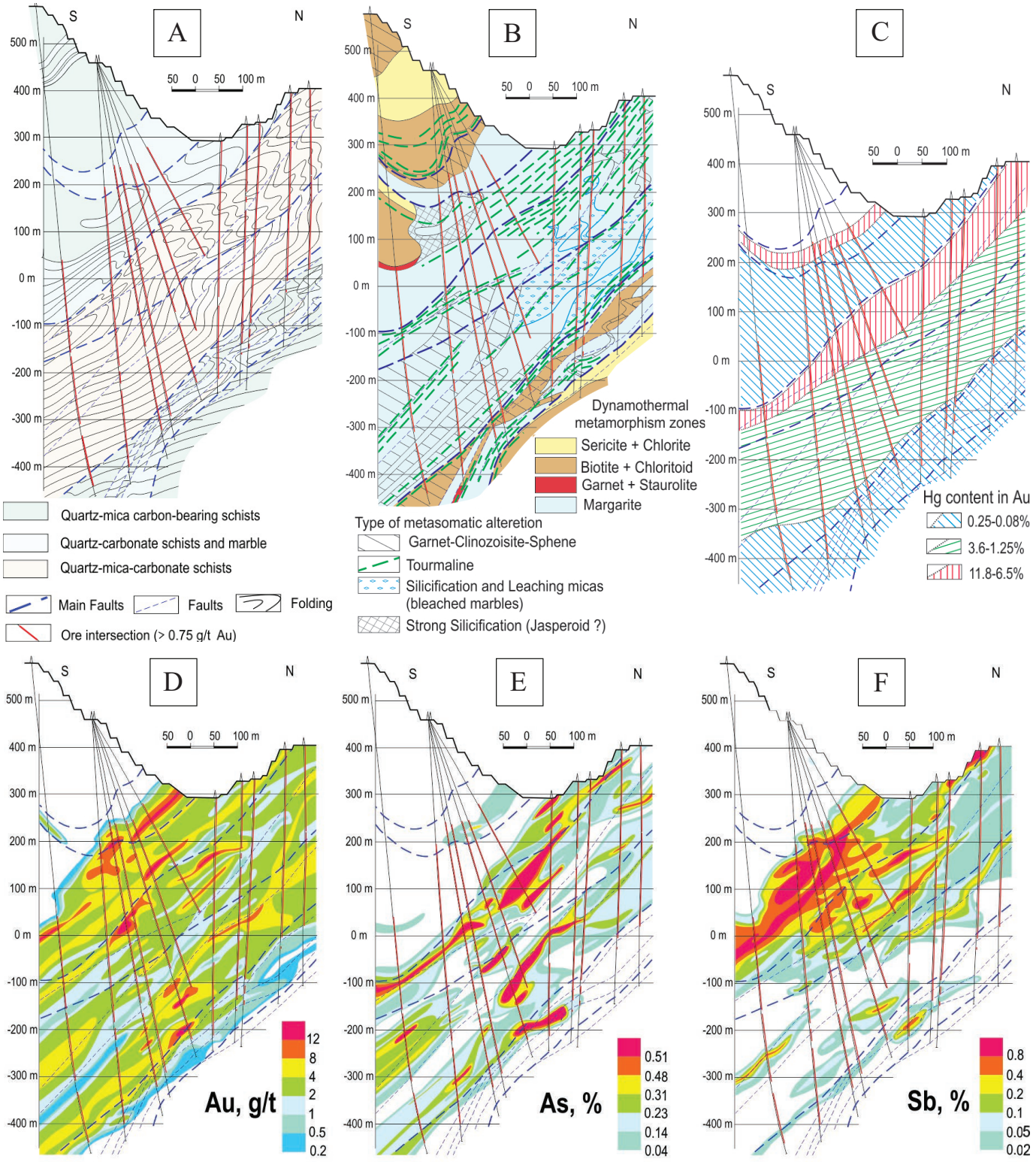

Fig. 7. Cross section of East Olympiada, alongline B-B' in Figure 6. A = structural-lithologic pattern; B = metamorphic and hydrothermal zonation; C = distribution of mercury in gold; D = distribution of gold; E = distribution of arsenic; F = distribution of antimony.

The orebody is saddle-shaped and plunges steeply south at 65° to 75°, swelling near the fold closure and irregularly mineralized along the limbs (Fig. 6). The orebody is banded, concordant with the axial planar structural fabric, with alternation of high- and low-grade bands of variable thickness following the bedding. The ore contains 2 to 7 vol % sulfide, with gold grades varying from 0.2 to 165.4 g/t and averaging ~4 g/t Au. There are local stratiform mineralized shoots grading 5.8 to 8.6 g/t Au, a few tens of meters in vertical and horizontal extents. Such shoots occur at the intersections of tectonic zones with complex internal folding and lithologic contacts where they are intensely mineralized with arsenopyrite and stibnite.

Away from the fold closure, there are two orebodies along the southern and northern limbs of the antiform (Fig. 6). In the north, predominantly disseminated gold-arsenopyrite mineralization occurs mostly in mica-quartz-carbonate schist. In the south, disseminated mineralization occurs mainly in tectonized banded marble, 150 m thick, and extends upward into tectonized carbonaceous schist. The disseminated mineralization along the south limb is of gold-antimony type, with insignificant arsenopyrite.

The drill-proven vertical extent of mineralization exceeds 1,400 m, remaining open downplunge and maintaining the grade. In 2016, Polyus estimated a resource of 79.5 Mt @ 5.55 g/t Au for 441.6 t Au below the planned open pit (between –60mRL and –570mRL).

East Olympiada differs from other zones in the volume of its oxidized ore. It developed to a 400-m depth, giving rise to some of the deepest supergene oxidation in the world. At surface, the 45,000-m² orebody was completely oxidized except for its eastern part. The auriferous oxide is column-shaped in vertical section (Fig. 2B, C), completely disappearing at +280mRL. Gold grade reaches 447.2 g/t in the oxidized orebody, averaging 11.1 g/t.

Characteristics of mineralized rocks

The deposit is hosted in metamorphosed rocks of the Korda Formation. From top to base, these are carbonaceous quartz-mica schist, foliated marble, quartz-mica-carbonate schist, and biotite-muscovite-quartz schist (Fig. 6). Chemical composition of the rocks ranges from aluminous to carbonate-rich, with minor variation in ferromagnesian content.

All rocks are hydrothermally altered to different degrees and contain sulfide mineralization. The principal host rocks are quartz-mica-carbonate (two mica-quartz-calcite) schist and marble. In the underlying quartz-mica (quartz-garnet-mica) and overlying quartz-mica-carbonaceous (carbonaceous silicate) schists, mineralization occurs only near the contacts with carbonate-bearing and carbonate rocks.

Carbonaceous quartz-mica (carbonaceous sericite-quartz and carbonaceous biotite-chloritoid) schist: This schist is black with lens-shaped schistosity and is essentially a blastomylonite with lithic clasts a few millimeters in size (Fig. 8A). The schist consists of sericite-muscovite (20–50%), quartz (25–40%), graphite (5–10%), and chloritoid (5–25%). Graphite dusting follows cleavage planes. Tourmaline, ilmenite, rutile, pyrite and pyrrhotite are always present (up to 10%), whereas staurolite, garnet, biotite, plagioclase and calcite are only locally present. Lenses of clinozoisite-carbonaceous schist are present in carbonaceous rocks and quartz-bearing marble, with clinozoisite making 10 to 30% of the rock.

The two mica-chloritoid carbonaceous blastomylonite near faults is intensely silicified and impregnated with auriferous arsenopyrite and stibnite mineralization, accompanied by quartz recrystallization and minor chloritization of biotite.

Foliated marble: This marble is a gray banded rock (Fig. 8B) with a fine-grained equigranular texture. The rock consists predominantly of calcite, with 5 to 10% quartz, muscovite, chlorite, margarite, and dusty graphite. Pyrrhotite is everywhere present, with smaller amounts of pyrite. The amount of granoblastic quartz in mineralized rocks increases to 15 to 30%. Mineralization occurs as fine sulfide disseminations and clustered veinlets. Needle and isometric arsenopyrite developed in fine-grained rock. Dusty graphite, rutile, stibnite, and berthierite occur between the arsenopyrite grains. Sulfide clusters consist of pyrite, stibnite, berthierite, pyrrhotite, chalcopyrite, sphalerite, and native antimony. Sulfides are accompanied by silicification and coarse-grained aggregates of calcite and quartz. Fibrous graphite also follows the schistosity, along with disseminations of arsenopyrite, stibnite, pyrrhotite, and pyrite.

Quartz-mica-carbonate (two mica-quartz-calcite) schist: This schist is pale green, sometimes brownish. The rock is finely (0.5–2 cm), medium (5–10 cm), and thickly (50–80 cm) banded (Fig. 8C, D), with moderately to well-developed schistosity. The rock consists of calcite (15–40%), quartz (10–40%), plagioclase (5–20%), muscovite (5–25%), biotite (5–35%), margarite (up to 1%), tourmaline (1–3%), rutile (3–5%), and sulfides (3–10%). The sulfides occur along relict banding planes in schist that locally contains parallel lenses of silicified and sulfidized marble. The texture of rocks is fine-grained to sucrose. Muscovite, relict plagioclase, chlorite, and margarite do not make up more than 10% of rock volume, with trace very fine rutile and rare pale-green tourmaline and apatite. In "bleached" alteration zones, there are calcite (~50 vol %), quartz-calcite (~10%), and quartz (~40%) segregations, accompanied by sulfide segregations, from a centimeter to a few tens of centimeters long. There is a progression of metamorphic assemblages with increasing alteration and mineralization. The primary metamorphic paragenesis comprises quartz, calcite, andesine, biotite, muscovite, margarite, and chlorite. Calcic alteration with garnet, clinozoisite, sphene, albite, and K-spar was possibly close in time to late stages of the metamorphism. Near mineralization, the schist is altered to silica and to titanite, clinozoisite, quartz, and calcite. Where gold mineralized, the schist also contains muscovite, quartz, and sulfides. Areas with elevated concentration of muscovite (up to 25%) have coarse pseudomorphs of this mineral after biotite, with some biotite preserved. This progression in metamorphic paragenesis ends in sulfidization, with deposition of early pyrrhotite and pyrite, impregnation of needle arsenopyrite, and negligible antimony mineralization. Arsenopyrite is common in biotite, but there is no specific correlation between arsenopyrite and biotite.

Later (intramineral) silicification destroyed the primary assemblage and dissolved and partially redeposited clinozoisite, titanite, and garnet, with crystallization of labradorite-anorthite and recrystallization of quartz (with small input of additional SiO_2) and calcite (with appearance of

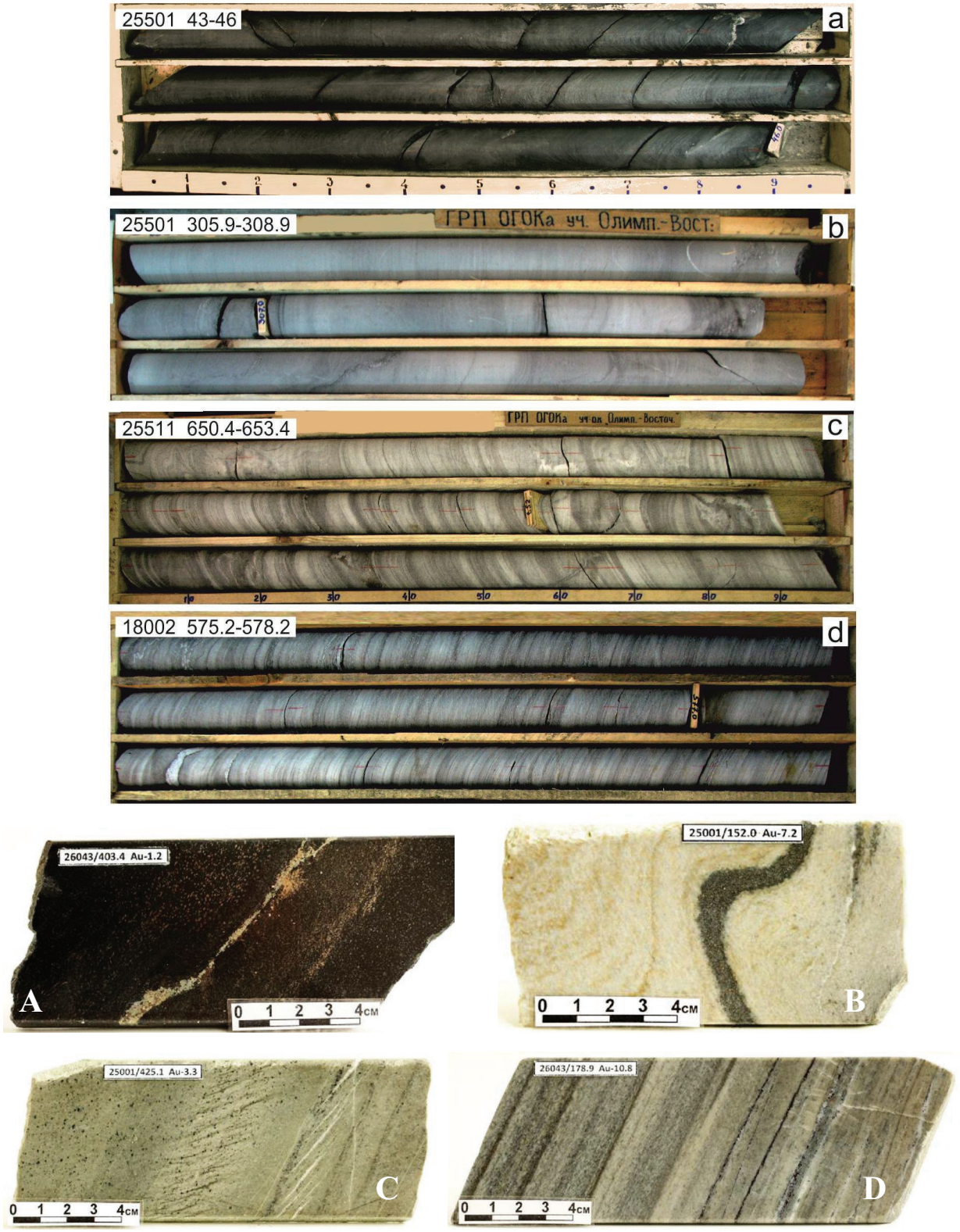

Fig. 8. Principal host-rock types of Olympiada deposit. Drill core: a = carbonaceous blastomylonite from drill core with lensoid schistosity, b = foliated marble, c = two-mica quartz-calcite schist, d = garnet-two mica-quartz schist. Hand samples: A = carbonaceous sericite-quartz schist with disseminated pyrite, pyrrhotite, arsenopyrite, chalcopyrite, sphalerite, and tetrahedrite; B = quartz-bearing marble with bands of disseminated pyrrhotite, pyrite, arsenopyrite, minor chalcopyrite, and ulmannite; C = quartz-mica-carbonate schist with cleavage and disseminated pyrrhotite-pyrite-arsenopyrite; D = banded quartz-mica-carbonate schist with pyrrhotite-arsenopyrite-antimony mineralization. Numbers in photos are drill hole numbers, depth of sample (m), and gold grade (g/t).

dolomite and formation of calcite-sericite pseudomorphs after andesine).

Late-stage sulfide minerals tend to occur in quartz-calcite aggregates and consist of sphalerite-galena and gersdorffite-ulmanite. There are also common microscopic grains of gold, aurostibite, and tellurides. Sulfides are accompanied by enlarged grains of calcite, quartz, and rutile. Needle arsenopyrite is absent from these aggregates, which rather contain newly formed, asterisk-like and dipyramidal arsenopyrite crystals associated with pyrite and pyrrhotite. Practically everywhere, calcite veins are accompanied by millimeter-sized berthierite grains.

Biotite-muscovite-quartz (or garnet-two mica-quartz) pale-green to brownish schist: This schist constitutes the lower part of the host sequence in the core of the recumbent folds. The schist is a banded (0.1–>10 cm) rock. About 50% of the sequence is deformed into meter-scale folds. The garnet-two mica schist includes boudinaged and mylonitic rocks. There is common cleavage in combination with microfolds and microlensing. Mineralogically, the schist consists of biotite (15–35%), muscovite (5–40%), and quartz (20–40%). Purple almandine and green chlorite are present in a fine-grained groundmass. Garnet is regularly present, forming 3 to 5% of the rock volume. Quartz and sericitized plagioclase make up 5 to 30% of rock volume, with carbonate up to 5%, mainly due to carbonatization. The accessory minerals are tourmaline (<2%), apatite (<1%), pyrite, and pyrrhotite, with the latter twice as abundant as pyrite. Ilmenite (up to 3%) is constantly present but its concentration decreases as sulfides increase. In the orebodies, the rock is silicified and muscovitized, albeit macroscopically not visually distinct from barren rock. The altered rocks typically contain carbonate, both in the rock mass and veins. Garnet is almost everywhere replaced by chlorite. Concentrations of biotite decrease, and it almost disappears, where muscovite forms 60 to 70% of the rock. Poikiloblastic titanite is associated with pyrrhotite, with the latter crosscutting the former in places. There are rare idioblastic arsenopyrite needles in titanite.

The quartz-garnet-two mica schists rarely host economic mineralization, which is mostly present as small disseminated and lens-shaped pyrrhotite aggregates along the schistosity planes. Pyrrhotite associates with arsenopyrite, chalcopyrite, rutile, and titanite. Chalcopyrite is present in pyrrhotite and in gangue minerals in combination with pyrrhotite. Arsenopyrite needles are irregularly distributed in gangue minerals, forming rare single idioblasts and richly disseminated glomeroblastic aggregates in sulfidized rock. Arsenopyrite was found inside pyrrhotite and associates with pyrite, forming single grains (0.1–0.3 mm) and aggregates.

Metamorphism and hydrothermal alteration

Sedimentary rocks are regionally metamorphosed to epidote-amphibolite facies of andalusite type (Zvyagina, 1989; Likhanov et al., 2004). Mineral assemblages are garnet-muscovite-biotite, developed after siltstone.

The area of the Olympiada deposit has a local zone of dynamothermal metamorphism and alteration, characterized by distinct mineral assemblages, and spatially restricted to the long-lived tectonic zone along the mineralized horizon, comprised of chemically reactive carbonate rocks and ductile carbonaceous shale. This zone generally mimics the fold structure hosting the deposit (Figs. 5C, 6) and its boundaries are subparallel to the lithologic units, although not fully coincident.

The limbs consist of predominantly greenschist facies rocks (sericite + chlorite and biotite zones, T = 400°–420°C, P = 3–4 kbars), which occur symmetrically relative to the axis of the Medvezhinsky fold. The sericite and chlorite zones are controlled by the carbonaceous stratigraphic unit. A 420° to 450°C temperature of metamorphism was defined using the concentration of titanium in biotite (Henry et al., 2005). In the axial part of the zone and fold closures are the epidote-amhibolite metamorphic facies. The highest temperature associations of metapelites in the tectonic sliver correspond to the garnet zone (garnet + quartz + biotite ± plagioclase), with sporadic fibrolite-sillimanite and kyanite. Higher pressure rocks correspond to the kyanite type of metamorphism, with mineral associations of chloritoid + biotite ± garnet (in metapelite) and margarite + quartz (in metamarl). The temperature defined by the garnet-biotite thermometer (Holdaway, 2000) is 580° to 605°C, with 590° to 595°C defined by the biotite thermometer (Henry et al., 2005). The pressure defined using the garnet-biotite-plagioclase-quartz barometer (Wu et al., 2004) is 7.2 to 7.5 kbars.

Within this zone of distinct metamorphic and alteration assemblages, there are diverse auriferous hydrothermal mineral associations (Fig. 7b; Li, 2003; Serdyuk et al., 2010; Borisenko et al., 2014), reflecting variable lithology of the host rocks and multiple hydrothermal events. The products of calcic and acidic silica alteration, sometimes with abundant rutile, tourmaline, graphite (bitumen), and sulfidization, are the most typical. Gold associates with sulfides.

Widespread calcic alteration developed in mylonite zones and in lithologically contrast carbonaceous, carbonate, silicate-carbonate, and silicate host rocks. Macroscopically, this alteration is not recognizable and takes the appearance of unaltered rock with preserved relic bedding, color, and grain size, but with newly formed clinozoisite, zoisite, titanite, garnet, K-feldspar, and albite.

Acidic alteration produced patchy silicification in carbonate and carbonate-bearing rocks, which is difficult to trace between adjacent drill holes. Within the orebodies are the predominantly calcite rocks, probable products of carbonate remobilization into the margins of silicified rocks. The bleached, silicified marble is a product of acidic leaching of Fe-Mn rock-forming minerals, interpreted to be synchronous with mineralization (after needle arsenopyrite and before galena-sphalerite). This alteration has much in common with jasperoid, although silicification of carbonates is not fully developed.

In addition, tourmaline forms bands along the schistosity planes, faults, and folds in the schist unit (Fig. 7b). It is a mixture of dravite, uvite, and schorl, forming small irregularly oriented idiomorphic crystals. The boron metasomatism is interpreted to have developed before the gold mineralization and does not correlate well with gold.

Sulfidization plays a main role in formation of the Olympiada deposit, gold being intimately associated with disseminated sulfides in the rocks and sulfidic microfractures. Auriferous hydrothermal alteration consists of muscovite-quartz-calcite, with significant variation of proportions of these minerals. The

associated sulfide minerals are practically identical at all sites. The gold-bearing mineral is needle arsenopyrite, present in locally developed early skarnoids and quartz-carbonate (with clinozoisite), silica, and carbonate alteration. However, there is no correlation between intensity of alteration and abundance of arsenopyrite.

Hydrothermal alteration associations (clinozoisite+titanite in metapelite and garnet + clinozoisite + titanite in metamarl) record temperature of 320° to 480°C and pressure of 1.3 to 3.5 kbars (Winkler, 1979). Temperature of formation for muscovite from quartz-muscovite-carbonate alteration near the orebodies, defined using the paragonite-phengite geothermobarometer (Dobretsov, 1977), is 290° to 380°C and pressure is 1.0 to 3.5 kbars as products of acidic metasomatism.

Gas chromatography and mass spectrometry identified aliphatic, cyclic, oxygen-bearing and heterocyclic hydrocarbons in quartz from veins and ore-bearing alteration. However, it is not clear what role was played in mineralization by hydrocarbons, such as methane, naphthene, aromatic resins, and asphalthene, as identified at East Olympiada (0.02–0.06%) in association with auriferous sulfides by means of luminescence.

The latest low-temperature alteration took place under the influence of meteoric water. It produced illite-quartz in the most tectonically disturbed part of the deposit. It is possible that supergene oxidation was coeval with low-temperature argillization. Such oxidized zones are anomalously rich in Au, W, and Pb, and are traditionally viewed as a weathering crust or gold-bearing regolith in Russia. According to Storozhenko et al. (2002), the oxidized zone at Olympiada hosts Paleogene-Quaternary spore-pollen spectra at a depth of 5 to 28 m, gradually changing to Mesozoic spectra at 30- to 60-m depth, and Late Devonian, Carboniferous, and Permian types at a depth of 50 to 110 m.

Gold mineralization

Hypogene and supergene mineralization are compositionally very different at Olympiada, which translates into different responses to beneficiation (Bernatonis, 1999; Li, 2003).

Hypogene sulfide ore: The hypogene sulfide ore constitutes the bulk of the deposit. The mineralization contains 2 to 7 vol % sulfide in quartz-mica-carbonate alteration. The main gangue minerals are 35 to 40 vol % carbonate (calcite, ankerite), 30 to 43 vol % quartz, mica (8–10 vol % muscovite, 10–15 vol % biotite) and a few vol % magnesian chlorite.

The ore minerals form fine aggregates of pyrite, pyrrhotite, arsenopyrite, stibnite, berthierite, and rare native gold in association with antimony sulfides (Table 2). Most ore minerals, including native gold, are microscopic. Gold grade in ore varies from 0.2 to tens of grams per ton, locally attaining kilograms per ton.

The bulk chemical composition of sulfide ore reflects the bulk mineralogic composition of the host rocks with SiO_2, CaO, Al_2O_3, CO_2, MgO and Fe_{tot} as the major components (Table 3). The concentrations of these components, as well as As and Sb, are widely variable. Gold is the main economic metal, with by-product silver and antimony.

Gold in hypogene sulfide ore is fine to "dusty." The dominant size of gold particles is 10 μm, but some individual grains reach 1 mm. There is about 15% free gold in samples crushed to –0.074 mm. Micron-sized native gold occurs as inclusions in quartz (35%), arsenopyrite (35%), pyrite, and marcasite (15%), pyrrhotite (5%), berthierite and stibnite (5%), carbonate (5%), and less commonly in gudmundite, chalcopyrite, tetrahedrite, gudmundite-pyrrhotite simplectite, and muscovite (Fig. 9). Up to 45% of sulfide-hosted gold is cyanide treatable and about 39 to 60% of it is refractory but can be treated after biooxidation (Sovmen et al., 2009).

Table 2. Mineral Composition of Hypogene Sulfide Ores from Olympiada

Group	Mineral	Amount (wt %)
Gangue	Carbonates (calcite, siderite, dolomite)	41–55
	Quartz	36–56
	Mica: sericite, muscovite, biotite, margarite, chloritoid	1.0–6.7
	Fluorite	Traces
	Graphite	Traces
	Rutile	Traces
	Ilmenite	Traces
	Magnetite	Traces
	Hematite	Single grains
Sulfides	Arsenopyrite	0.6–2.1
	Pyrrhotite	0.06–1.0
	Chalcopyrite	Traces
	Galena	Traces
	Sphalerite	Traces
	Cobaltite	Traces
	Gersdorffite	Traces
	Cinnabar	Traces
	Pyrite	Traces
	Marcasite	Traces
	Melnikovite	Traces
	Bismuthinite	Traces
	Alabandite	Traces
	Pentlandite	Traces
	Violarite	Traces
	Molybdenite	Traces
	Cubanite	Traces
	Valeriite	Traces
	Bornite	Traces
	Cobaltine	Traces
	Mackinawite	Traces
Antimony minerals	Stibnite	0.03
	Gudmundite	Traces
	Berthierite	Traces
	Plagionite	Traces
	Ulmanite	Traces
	Williamite	Traces
	Costibite	Traces
	Breithauptite	Traces
	Chalcostibite	Traces
	Bournonite	Traces
	Jamesonite	Traces
	Nisbite	Traces
	Tetrahedrite	Traces
Native	Gold	Up to 4 g/t
	Aurostibite	Traces
	Antimony	Traces
	Lead	Traces
	Mercury	Traces
Tellurides	Bismuth tellurides	Traces
	Altaite	Traces
	Coloradoite	Traces
Tungsten minerals	Scheelite	Traces
	Wolframite	Traces

Table 3. Chemical Composition of Au-As Sulfide Ores at Olympiada (wt % avg of bulk metallurgical samples by Polyus Gold)

SiO_2	TiO_2	Al_2O_3	Fe_{total}	MnO	MgO	CaO	K_2O	Na_2O	P_2O_5	S_{total}	S_{sulf}	CO_2	C_{org}	As	Sb	Au (g/t)
50.48	0.54	12.82	5.88	0.32	3.14	16.44	1.76	0.05	0.11	0.53	0.46	8.16	0.18	0.19	0.05	5.0

The shape of gold is irregular, platy, veinlet, droplet, and spongy. The fineness of gold is 910 to 997. It also includes silver, copper, and mercury (0.2–5.9%). Gold, where in association with stibnite and berthierite, has a spongy texture. It has a fineness of 647 to 757 and is a mixture of silver (15–22%) and mercury (9–13%). In addition, there is ferruginous, mercury-ferruginous, and cupriferous gold. Cupriferous gold associates with minerals of polymetallic association, whereas ferruginous and mercury-ferruginous gold occurs with the stibnite-berthierite mineralization.

Silver grades attain 2 to 3 g/t, in places as native silver, earthy argentite, and electrum. Gold- and silver-grade shells do not spatially coincide. Elevated silver was recorded in pyrrhotite and calcite veinlets, but silver mostly correlates with the base metal sulfide (Table 4) and stibnite-berthierite associations.

Stable mineral assemblages define a clear paragenetic sequence (Table 4). Early disseminated sulfides of gold-arsenic ores include arsenopyrite, pyrite, and pyrrhotite, which occur in silicified and muscovitized schist. Base metal sulfides occur as microscopic inclusions of chalcopyrite, sphalerite, galena,

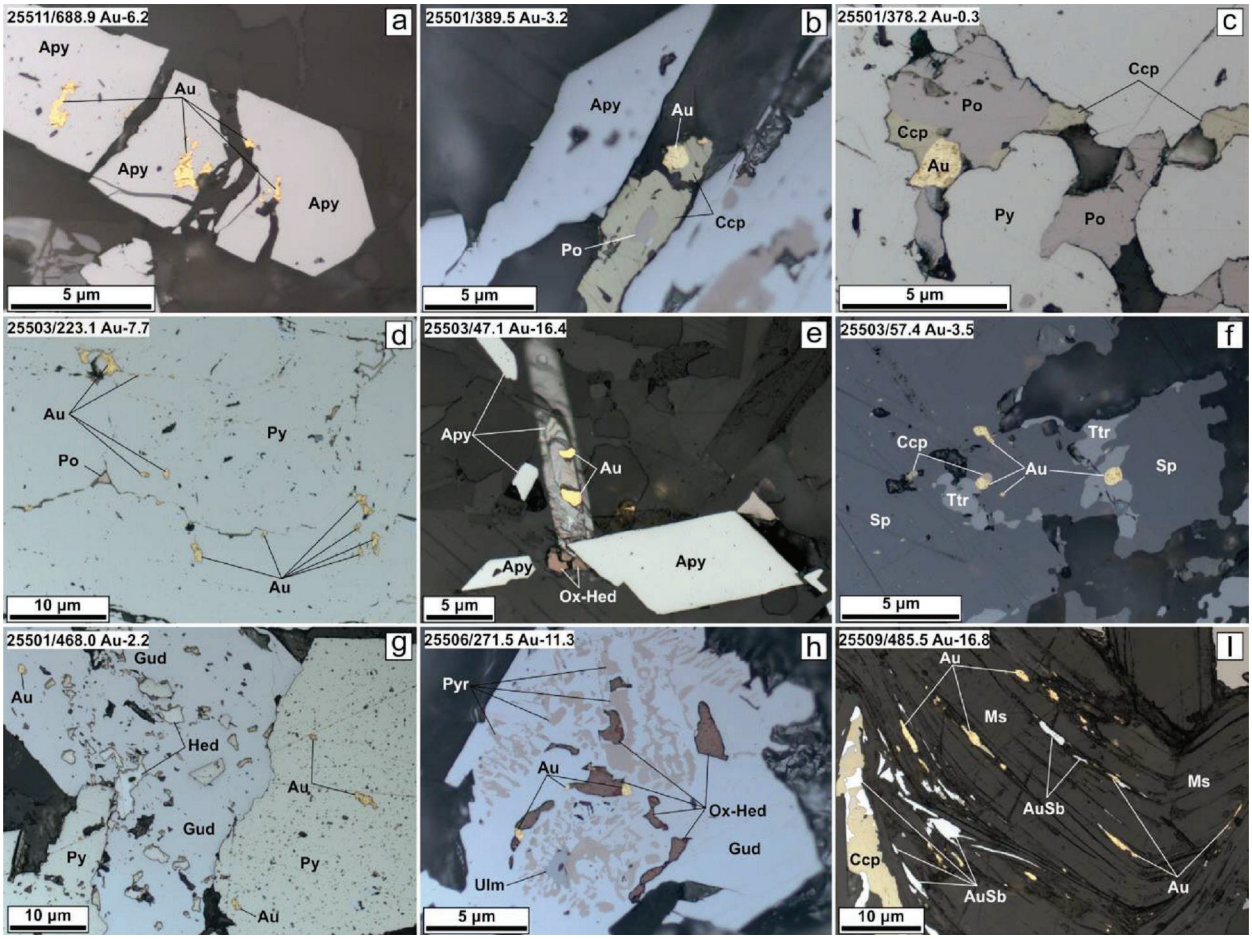

Fig. 9. Associations of gold mineralization: A-D = early sulfides of gold-arsenic association; E-I = associations of antimony stage. 25509/485.5 Au-16.8 = sample numbers (drill hole/depth), gold grade in g/t. Apy = arsenopyrite, Au = gold, AuSb = aurostibite, Po = pyrrhotite, Py = pyrite, Ccp = chalcopyrite, Ox-Hed = oxidized hedleyite, Ttr = tetrahedrite, Sp = sphalerite, Ulm = ulmanite, Ms = muscovite. A. Cataclastic crystal of prismatic arsenopyrite in quartz-carbonate matrix. Gold inclusions and fracture fillings in arsenopyrite. B. Association of arsenopyrite, pyrrhotite, chalcopyrite, and gold. Gold is intergrown with chalcopyrite. C. Aggregate of chalcopyrite, pyrrhotite, and gold as inclusions in pyrite. D. Gold in fractures in pyrrhotite and pyrite. E. Pseudodipyramidal and needle crystals of arsenopyrite in quartz-carbonate matrix. Gold and hedleyite (oxidized at the surface of polished section) on arsenopyrite. F. Sphalerite with fine inclusions of chalcopyrite and coarser inclusions of tetrahedrite. Gold occurs along the boundaries between sphalerite and tetrahedrite. G. Aggregate of pyrite and gudmundite metacrystals. Hedleyite forms amoeboid inclusions in gudmundite. Inclusions of gold in pyrite and gudmundite. H. Symplectic aggregate of gudmundite and pyrrhotite, with inclusions of ulmannite, hedleyite (oxidized at the surface of polished section), and gold (at the boundary between hedleyite and gudmundite). I. Elongate gold and aurostibite in joint cracks in muscovite. Aggregate of chalcopyrite and aurostibite to the left.

Table 4. Sequence of Mineralization at Olympiada (compiled by A.M. Sazonov)

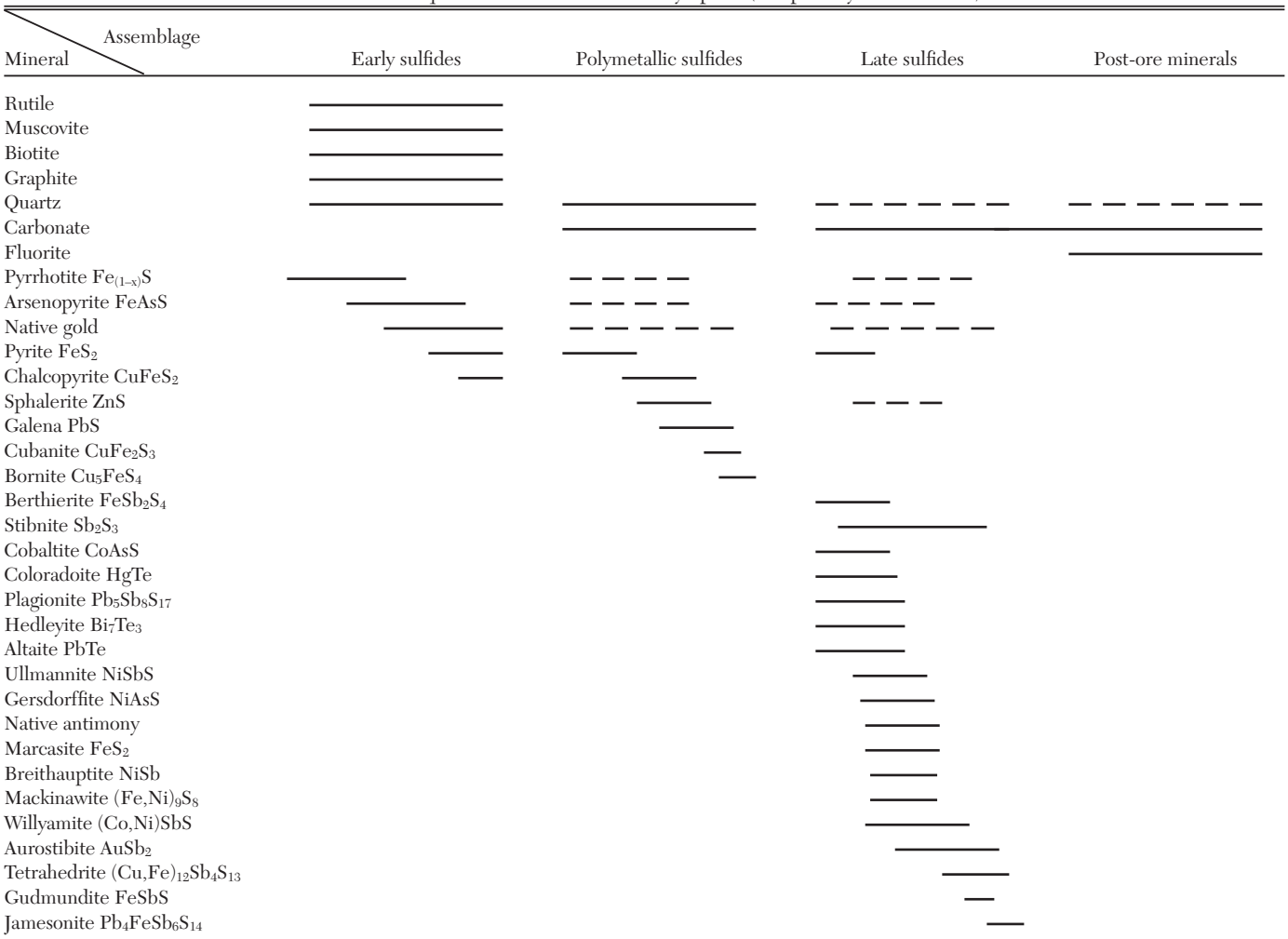

Note: Solid lines correspond to primary minerals, dashed lines are recrystallized minerals

and some tetrahedrite, overprinting the pyrite-arsenopyrite-pyrrhotite aggregates. These areas locally host visible gold. A late veinlet-disseminated gold-antimony (berthierite-stibnite) assemblage, with coarser and rarely visible gold and aurostibite, overprints the early sulfides, mostly in the south of East Olympiada, near the Medvezhyi fault. The spatial coincidence of several generations of sulfides corresponds to the highest grade, also supposedly associated with scheelite. Postore fluorite-carbonate veinlets are widespread but generally minor.

Ore minerals form banded disseminations along the cleavage planes and schistosity, with millimeter- to centimeter-thick veinlets and aggregates (Fig. 10). The structure of the ore is usually fine-grained metacrystalline, with traces of recrystallization and coarse-grained, clustered aggregates near quartz veinlet boudins in internal tectonic zones. The orebodies can be visually outlined by the appearance of concentrated aggregates of arsenopyrite, pyrite, pyrrhotite, and stibnite, but their boundaries can be drawn only based on assay results. The ores can be divided into gold-arsenic and gold-arsenic-antimony types. The minor minerals are rutile, titanite, wolframite, and scheelite, forming fine dissemination in most altered and mineralized rocks.

Gold-arsenic ores: The gold-arsenic ores consist mainly of early sulfides with minor overprinting polymetallic sulfides (Table 4), averaging 3.9 g/t Au. Sulfide mineralization is mainly represented by needle and finely prismatic arsenopyrite, pyrrhotite, and pyrite (Fig. 10A-E), with minor overprinting chalcopyrite, sphalerite, bornite, and cubanite. Arsenopyrite (0.1–5%, avg 1–1.5%) in this ore type forms fine disseminations in the main mica-quartz-calcite ore. The individual crystals vary from a few microns to 1.5 mm in length, most commonly intergrown with pyrrhotite. Its composition is 32 to 36% Fe, 41 to 48% As, and 19 to 23% S. The crystallization temperature, based on an S/As – S + As/Fe diagram (Sazonov et al., 2016) and geothermometer (Kretschmar and Scott, 1976; Scott, 1983), varies between 300° and 460°C, with $\log \alpha_{S_2} = -14.6$ to –5.9.

In carbonaceous quartz-mica schist, pyrrhotite prevails over arsenopyrite in general and, especially, in low-grade ore. It is widespread outside the deposits within the entire marker horizon and extremely uncommonly in underlying garnet-mica-quartz schist. Pyrrhotite (1.5–3% of the rock) forms bands, several millimeters to 7 to 8 cm thick, with coarse-grained aggregate structure (Fig. 10D). It also forms massive

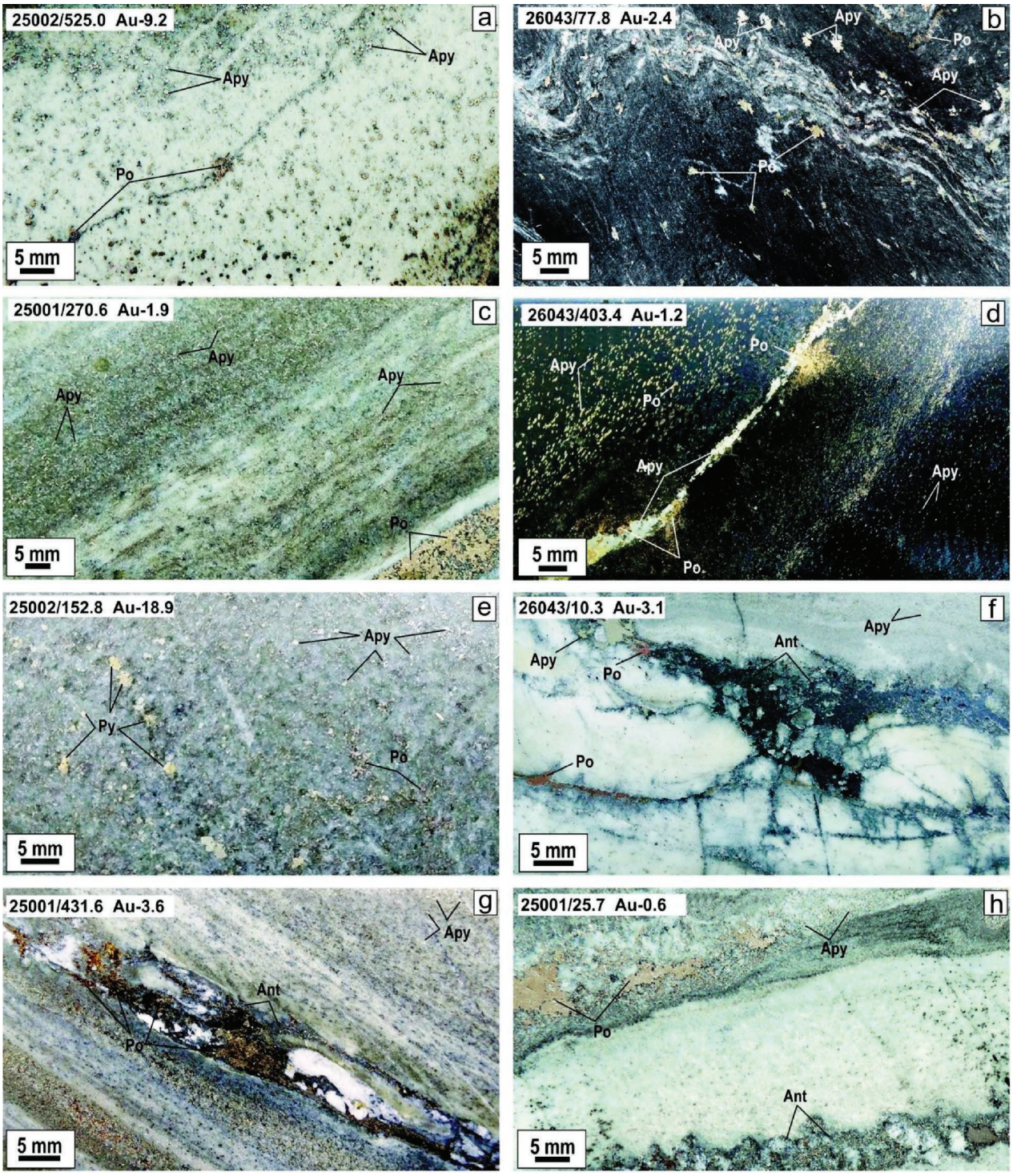

Fig. 10. Textures and structures of Olympiada ores. 25001/431.6 Au-3.6 = sample number (drill hole/depth), grade in g/t Au. a = crystalline disseminated arsenopyrite in mica-quartz-carbonate schist. Pyrrhotite in cleavage planes; b = crenulated carbonaceous blastomylonite with crystalline pyrrhotite and pseudodipyramidal arsenopyrite; c = irregular distribution of needle arsenopyrite in schist. Bottom right = veinlet aggregate of pyrrhotite; d = banded distribution of disseminated pyrrhotite-arsenopyrite in carbonaceous shale. Central quartz-carbonate veinlet contains pyrrhotite and arsenopyrite; e = disseminated pyrite-pyrrhotite-arsenopyrite in schistose marble; f = brecciated quartz vein, with stibnite-pyrrhotite-arsenopyrite in cement and along cracks; g = stibnite-pyrrhotite-carbonate veinlet in schist, with disseminated pyrrhotite and needle arsenopyrite; h = banded mica-quartz-carbonate schist with pyrrhotite and stibnite along cracks. Abbreviations: Ant = stibnite, Apy = arsenopyrite, Po = pyrrhotite.

coarse-grained accumulations on the margins of lens-shaped segregations of coarse quartz (Fig. 10H). The bulk of the pyrrhotite is interpreted to have crystallized at 400° to 420°C and log α_{S_2} = –19.9 to –0.8 (calculated using Toulmin and Barton, 1964; Lambert et al., 1998).

Microscopic gold particles occur in combinations of pyrite-pyrrhotite-arsenopyrite mineralization and polymetallic sulfides. Arsenopyrite material contains up to 4.7 kg/t Au (Genkin, 1998). Higher gold grade is recorded in sulfur-rich varieties of arsenopyrite that crystallized at 370-410°C and log α_{S_2} = –7.9 to –7.1. Gold is present within pyrrhotite as micron-sized inclusions in the central parts of arsenopyrite grains. The fineness of gold is 985 to 1,000 (Genkin, 1998; Genkin et al., 2002; Sazonov et al., 2016).

Gold-arsenic-antimony ores: The gold-arsenic-antimony ores contain mineralization of all stages (Table 5), with an average grade of 5.4 g/t Au. There is a diversity of intergrown minerals in association with stibnite, arsenopyrite, pyrrhotite, chalcopyrite, gold, and aurostibite (Fig. 9E-I), representing Co-As-S, Ni-As-S, Ni-Sb-S, Pb-Sb-S, Cu-Sb-S, Co-Sb-S, Hg-Te, and Bi-Te associations. The ores also contain stibnite and berthierite, with insignificant pyrite, marcasite, pyrrhotite, and isolated grains of native antimony, tetrahedrite, chalcopyrite, and jamesonite, in which gold grade decreases to 2.9 g/t, correlating with lesser concentrations of arsenic.

Pseudodipyramidal and short prismatic arsenopyrite grains, 5 mm across (Fig. 8E), contain 1.02% Sb, up to 2.96% Co, up to 0.74% Ni, and up to 0.07% Hg. This ore most commonly has microscopic and macroscopic gold in combination with antimony minerals and tellurides. Gold contains antimony (1–57%), copper (up to 41%), mercury (2–37%), silver (1–10%, rarely 25%), and nickel (0.8–3.7%). Some gold grains in this association reveal low fineness (734–825), but with high Sb (12.4–16.6%) and Ni (0.89–6.5%). Gold with anomalous mercury occurs at the base and top of the arsenic-antimony ores.

Oxidized ores: The oxidized ores (Table 6) are bright brown, red, dark gray, or orange in color (Bernatonis, 1999). They consist of scree (~10%), sand (~10%), silt (~16%), and clay (~64%). The main minerals are quartz (5–35%), illite (40–70%), iron hydroxides (1–36%), kaolinite (up to 14%), and chlorite (up to 10%). Minor and rare minerals include epidote, calcite, biotite, actinolite, chloritoid, clinozoisite, garnet, plagioclase, staurolite, sillimanite, zircon, rutile, anatase, brookite, and titanite. The primary ore minerals are gold, wolframite, scheelite, cinnabar, arsenopyrite, magnetite, stibnite, pyrite, and pyrrhotite. The supergene minerals are tungstite, hydrotungstite, scorodite and iron hydroxides, cervantite, valentinite, hydroromeite, skuokrikite, bindheimite, stibiokonite, as well as gypsum and barite.

Table 5. Gold in Mineralogical Types of Ore

Mineral association	Length (m)	Au (g/t)
Total interval	260	4.8
Ores with arsenopyrite and polymetallic sulfide	110	3.9
Ores including mineralization of all stages	116	5.4
Ores with stibnite+berthierite	34	2.9

The average gold grade in oxide is 2.3× higher than in hypogene ore, accompanied by a 1.7× decrease in specific gravity. About 38 to 62% of gold sits in the 9-μm clay fraction. Gold is free, as intergrowths with quartz and Fe, Mn, Sb, and As hydroxides, and as dispersed inclusions in secondary and relict primary minerals. The size of gold grains ranges from 0.071 mm (40–60%) to 0.1 to 0.25 mm (5–10%), with some particles up to 1 to 2.5 mm. Native gold (790–1,000 fine) constitutes about 64% of the ore. In addition to gold, oxidized ores contain tungsten (0.2–0.4% WO_3), which is poorly developed in the hypogene ore (Novozhilov et al., 2014).

Geochemistry of the ores

Nozhkin et al. (2011) showed that carbonaceous-clastic schists are regionally most enriched in gold (5–10 to 60 ppb Au). Sazonov (1998) estimated that average gold grade for the rocks of the Korda Formation is 1.1 to 1.3 ppb Au (for the lower greenschist facies), 4.3 to 5.8 ppb Au (in the dynamothermal metamorphic zones), and 15 to 249 ppb Au (for the host rocks near quartz veinlets within the deposit). The average grade of carbonaceous shales in the district is 26 to 47 ppb Au (Zvyagina, 1989), which are a potential source of gold to form Olympiada.

The Olympiada orebodies occur within large, low-grade gold envelopes which are several dozen meters across and extend for hundreds of meters vertically. They define an elongate oval shape, corresponding to the fold structure of the host rocks and strata-bound faults. In addition to gold, only arsenic, antimony, and tungsten form well-defined anomalies. Concentrations of Ag, Pb, Co, Ni, Mn, and Zn are also anomalous, but the shape of the anomalies is vague, and their size is much smaller than that for the three main pathfinders. The intensity and size of the geochemical halos depends on lithologic and physicochemical properties of the host rocks and structural-tectonic setting. The best and largest halos are developed around the orebodies in quartz-mica-carbonate schist and marbleized limestone, which are chemically active and physically permeable, and along the faulted contact with overlying quartz-mica-carbonaceous shale. Away from this contact and in poorly permeable carbonaceous quartz-mica schist, the intensity and size of the halos decrease. A similar pattern is observed in underlying quartz-garnet-mica schist.

At West Olympiada, the geochemical zonation from hanging wall to footwall of the orebody changes from As-Sb to Mn and to Au-W-Co-Ni-Pb-Mn. Downplunge, it changes from Au-As-Sb to W-(Co, Ni, Zn, Mn). At East Olympiada, the primary geochemical zonation (Fig. 7) is asymmetric (Li, 2003). The hanging-wall mineralized zone is dominated by Sb, As, Hg, and Mn. The footwall contains much less Sb and Hg, with

Table 6. Chemical Composition of Oxide Ores at Olympiada (wt %)

SiO_2	TiO_2	Al_2O_3	Fe_2O_3	FeO	MnO	MgO	CaO	K_2O	Na_2O	P_2O_5	L.O.I.
70.73–94.05	0.08–0.086	1.74–14.21	0.68–6.55	0.25–0.57	0.02–0.85	0.19–1.01	0.28–0.32	0.38–3.68	0.04–0.21	0.13–0.21	0.48–2.81

an increase in W, Co, Ni, and Pb content. Updip, there is an axial geochemical zonation from Au-As-Mo-Bi-W at –400mRL to Zn-Sn-(Ni, Co)-(Ti, Cu)-Sb-Ag at +100mRL. Geochemical halos in oxidized ores preserve the same zonation.

Genesis

Three main concepts that have been proposed for the source of gold, arsenic, antimony, and sulfur at Olympiada are: (1) synsedimentary (Petrov, 1974; Grigorov, 2003); (2) magmatic (Novozhilov and Gavrilov, 1999; Li, 2003; Korobeinikov et al., 2013); and (3) polygenetic, including metamorphic (Buryak, 1982; Sazonov et al., 2010; Serdyuk et al., 2010). Constraints on each of the events invoked by these concepts are examined below.

Age of host rocks and metamorphic events

The age of the host carbonate-clastic rocks of the Korda Formation corresponds to 1,450 ± 50 Ma (Sm-Nd data), whereas isotopic parameters of the Sm-Nd system (ε_{Nd} –6.1, TDM-2st 2,422 Ma) suggest erosion of early Paleoproterozoic greenstone belts (Nozhkin et al., 2008). Detrital zircons from this formation provide a maximum age of 1,580 Ma for sedimentation (Savichev et al., 2006). The K-Ar age of glauconite from sandstone of the overlying Pogoryui Formation is 1115 Ma (Shenfil', 1991).

Carbonate-clastic rocks of the Yenisei Ridge were overprinted by multiple metamorphic events. Likhanov et al. (2013) showed that initial low-pressure metamorphism, producing andalusite-bearing assemblages (metamorphic gradient dT/dH = 20°–30°C/km), took place around 1,050 to 850 Ma (Rb-Sr and Sm-Nd data). Metasediments were then metamorphosed to medium-pressure kyanite-sillimanite assemblages (dT/dH ≤10°C/km) in relationship to collision at 801 to 793 Ma. This corresponds to formation of blastomylonite along the shear zones (P 1.4–1.7 kbars, T 20°–30°C). This stage of metamorphism is viewed as coeval with the main gold event at Olympiada.

Exhumation metamorphism took place at 785 to 776 Ma in relationship to rapid uplift along shear zones (dT/dH ≤12°C/km), corresponding to the Tatarka-Ishimbino suture between the Central Angara and East Angara terranes (Fig. 3C). The origin of the suture is traditionally explained via collision between the two terranes (Vernikovskaya et al., 2016). However, the Central Angara and East Angara terranes are lithologically similar and ophiolites are present only in the southern segment of the suture, disappearing northward, and granitoids form a giant S-shaped cluster. This allows speculation about a sinistral (southward) translation of the Central Angara terrane and entrapment of the Meso- to Neoproterozoic ophiolites to the east, possibly in response to collision with the Isakovka terrane (Fig. 3A, C).

Age and source of magmatism

There are several stages in formation of magmatic complexes: ca 900 Ma (Teya-Eruda Complex), 760 to 718 Ma (Ayakhta and Glushikha Complexes), and 710 to 650 Ma (Gurakhta and Zakhrebetinsky Complexes). Petrochemical, geochemical, and isotopic characteristics indicate predominantly crustal origin of melts with some input from a mantle source (Vernikovskiy et al., 2006, 2016). The Gurakhta and, especially, Zakhrebetinskiy Complexes were formed from mantle-derived magma, contaminated by crustal material (Nozhkin et al., 2011; Vrublevskiy et al., 2017).

Near Olympiada, granitic intrusions are represented by the Tyrada and Chirimba massifs of the Ayakhta Complex. The $^{40}Ar/^{39}Ar$ age of granites from the Tyrada massif is 753.2 ± 5.5 Ma (unpub. data). The estimates of age of crystallization for the Chirimba massif vary from 840 ± 150 Ma (K-Ar method; Volobuev et al., 1973) to 868.9 ± 6.5 Ma (U-Pb on zircon; Sazonov et al., 2016) and 761.5 ± 8.0 Ma (U-Pb on zircon; Vernikovsky et al., 2003). The cooling of this massif to the closing temperature of the $^{40}Ar/^{39}Ar$ system of biotite took place at 721.4 ± 1.6 Ma (Vernikovsky et al., 2003).

Age of mineralization

More than 50 estimates for the age of mineralization exist for the Olympiada deposit based on the K-Ar, $^{40}Ar/^{39}Ar$, Rb-Sr, Sm-Nd, and Re-Os techniques. They range from 921 to 510 Ma (Sazonov, 1998; Novozhilov and Gavrilov, 1999; Li, 2003; Savichev et al., 2006; Sazonov et al., 2010, 2016; Nozhkin et al., 2011; Yakubchuk et al., 2014; Borisenko et al., 2014).

The work of the Novosibirsk Analytical Centre for Multi-Elemental and Isotopic Research at the Siberian Branch of the Russian Academy of Sciences was used for thermo-geochronologic reconstructions based on K-bearing minerals (sericite and muscovite) from mineral associations with different gold values, ranging from nonauriferous quartz-mica-sulfide assemblages to gold orebodies and antimony associations.

$^{40}Ar/^{39}Ar$ studies were conducted on 16 samples collected from nine drill holes at a depth of 39 m (drill hole 503) to 718.5 m (drill hole 510) from the richest Orebody 4 at East Olympiada. The age of the nonauriferous quartz-mica-sulfide mineral association is 817.1 ± 6.3 to 808.4 ± 7.7 Ma. The age of the main productive quartz-gold-arsenopyrite-pyrrhotite association is 803 ± 6.1 to 758 ± 6.0 Ma, with a prevalence of 795 to 784 Ma. The age estimates of the late quartz-gold-antimony association range from 795.2 ± 5.8 to 660 ± 19 Ma.

Li (2003) obtained K-Ar age estimates of 811, 765, and 754 Ma. Sazonov (1998) published K-Ar ages for mineralization of 877 to 771 Ma (muscovite) and 856 to 792 Ma (biotite). Rb-Sr data on sericite-(muscovite)-quartz-alteration, associated with the early productive gold-arsenopyrite mineralization, and quartz-sericite alteration of the late berthierite-stibnite association revealed a 794 ± 15 Ma isochron age for early alteration and 615 ± 15 Ma for late alteration (Novozhilov and Gavrilov, 1999). The Re-Os age of recrystallized arsenopyrite aggregates in association with stibnite mineralization is 689 ± 28 Ma (Borisenko et al., 2014). The Re-Os age estimates for coarse-prismatic arsenopyrite are 714 ± 36 Ma, and 750 Ma based on $^{40}Ar/^{39}Ar$ data. This contrasts with 511 ± 24 and 513 ± 40 Ma Re-Os estimates for pyrrhotite (Yakubchuk et al., 2014) that could be due to incomplete understanding of the Re-Os system in this pilot study. This wide range of ages suggests that hydrothermal activity at the Olympiada deposit could have continued for >150 m.y., from 817 to 660 Ma, broadly overlapping with the ages of magmatic activity. Mineralogically, we clearly observe the Au-Sb (berthierite-stibnite) association superimposed onto the earlier Au-As association.

Geochemical and isotopic studies

Lead isotope studies: Studies of Olympiada sulfide mineral associations (LA-ICP-MS, VSEGEI) revealed that lead from different mineral stages is distinctly different in isotopic composition and model age (Fig. 11A). The Au-Sb mineralization differs from Au-As ore in low $^{206}Pb/^{204}Pb$ ratio, pointing to depleted source in ^{238}U, unrelated to granitoids (Savichev et al., 2006). This could be a mantle isotopic reservoir that correlates with presence of mantle helium in the ore-forming fluids, which deposited stibnite and berthierite together with Hg-bearing gold. Mercury may also point to a mantle source. The fluids that produced the antimony associations are specific in their metal content (Rb, Ba, Sr, Cs, Mn, Ni), which may suggest an affinity of Au-Sb mineralization with similar-age alkaline and alkaline-mafic magmatism.

Sulfur isotope studies: Kryazhev (2017) showed that sulfur outside the orebodies is of sedimentary-diagenetic origin. Sulfides from carbonaceous shales reveal negative $\delta^{34}S$ (–21.8‰), whereas carbonate rocks show positive $\delta^{34}S$ values (+21.8‰), with maximum variations recorded at the boundary between the two units. In the orebodies, sulfur isotopes show two main populations (Fig. 11B). The preore pyrrhotite shows a well-defined peak at 7 ± 2‰ $\delta^{34}S$. Two types of arsenopyrite are shown in Figure 11A, C, D. Coarse-grained arsenopyrite-2 associated with low-grade ore has similar isotopic characteristics to preore pyrrhotite. In contrast, early needle arsenopyrite-1 and later stibnite associated with high-grade ore show a well-defined peak at 4 ± 5‰ $\delta^{34}S$.

Osmium isotope studies: Studies were conducted at Curtin University, Perth, Australia. The Os and Re values were recalculated taking into account the accumulation of radiogenic ^{187}Os after decay of ^{187}Re since formation of the minerals at ca 650 Ma (Fig. 11C, D). The $^{187}Os/^{188}Os$ values in needle

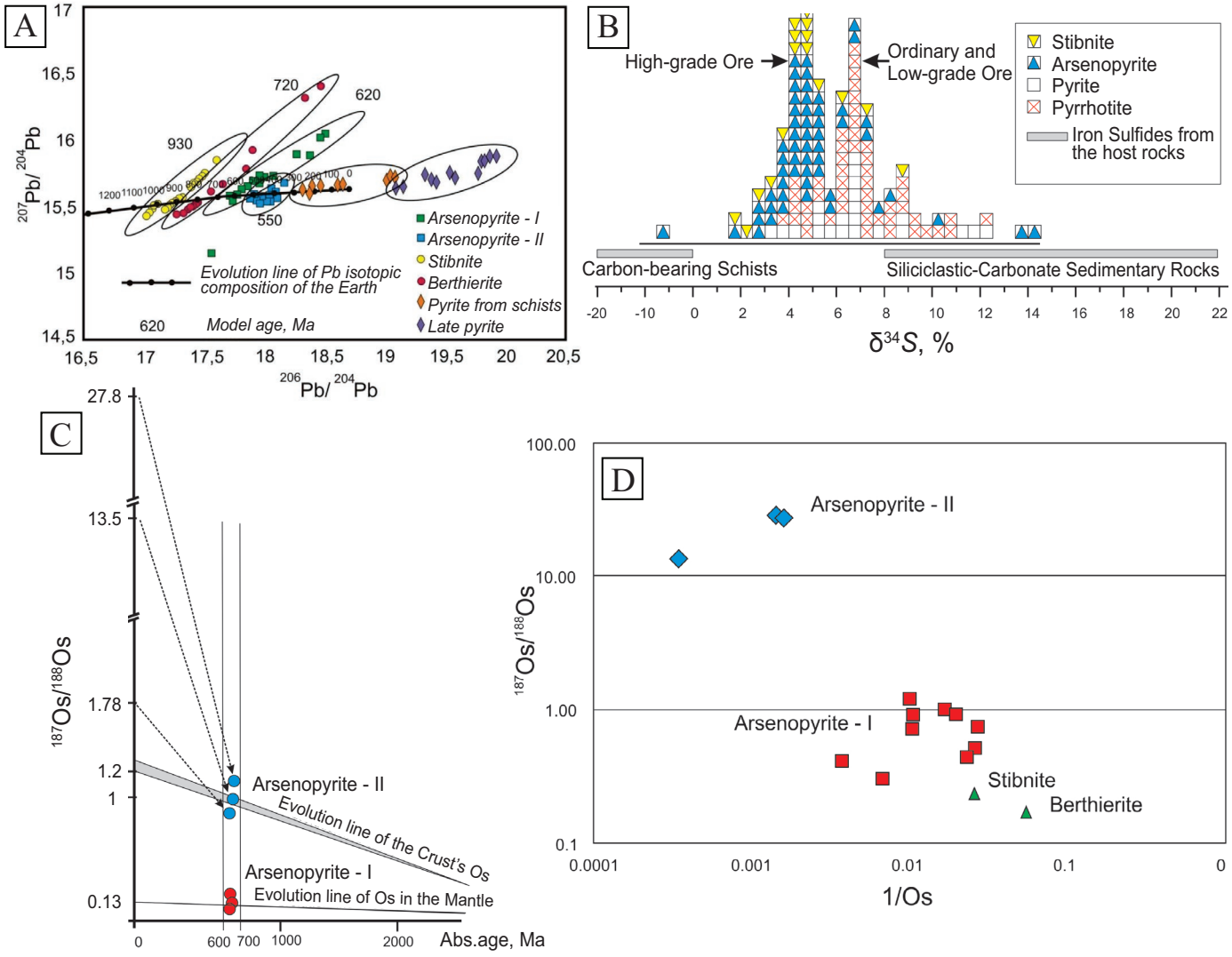

Fig. 11. A. Isotopic composition of lead from ore and rock at Olympiada (Savichev et al., 2006). Trends in isotopic composition of lead in needle arsenopyrite-1, berthierite and stibnite correspond to the mixing lines of mantle and crustal lead. This points to polygenic source in contrast to coarse arsenopyrite-2 with insignificant variation of values, pointing to a single crustal source. B. Isotopic composition of sulfur at Olympiada (Kryazhev, 2017). C. Os isotope composition in Olympiada sulfides: Os isotope composition of arsenopyrite-1 and arsenopyrite-2 at 0 Ma, calculated using the accumulation of the radiogenic component at 600 to 700 Ma (left); D. $^{187}Os/^{188}Os$ to 1/sum of all Os isotopes points to mantle/crustal source (Naumov et al., 2015).

arsenopyrite-1 are 0.35 to 0.11, which is 75 to 90% of mantle values. The $^{187}Os/^{188}Os$ values in coarse short prismatic arsenopyrite-2 are distinctly different (>10), corresponding to crustal values (Naumov et al., 2015) and consistent with its Pb isotope composition (Fig. 11a). Osmium in arsenopyrite-2 could be sourced from crustal granitoid melts or such osmium could be incorporated into fluids from the metamorphic or magmatic country rocks.

Helium isotope studies: The helium isotope studies were completed in fluid inclusions in quartz, stibnite, arsenopyrite-1, and arsenopyrite-2 (Gibsher et al., 2019). The fluids from short prismatic arsenopyrite-2 inclusions in quartz reveal crustal (<0.035*10^{-6} He), mantle, and even atmospheric values. A similar composition is typical for fluids from early metamorphogenic veins. Fluids from elongate prismatic arsenopyrite-1 in quartz and veins with pyrrhotite, berthierite, and Hg-rich gold, as well as in stibnite, are enriched in the light helium isotope. The $^{3}He/^{4}He$ values in these samples are 2.9, 3.25, and 2.1 (n*10^{-6}), which exceed crustal (<1) and atmospheric (1.4) values due to presence of mantle helium, with 10*10^{-6} values.

Rare earth element studies: Studies in sulfides (arsenopyrite, pyrite, pyrrhotite) and native gold revealed different patterns relative to unaltered rocks of the Korda Formation. This suggests a loss of metals from the rocks during mineralization (Kun et al., 2014). Prevalence of LREE and anomalies for Ce and Eu suggest a metamorphogenic origin as well as changes in Y/Ho, which correlate with the values for regionally metamorphosed rocks (Volkov et al., 2016). Some of the samples (arsenopyrite, pyrite, gold) reveal different patterns from the host rocks. This points to a possible contribution from a fluid of different origin due to inverse correlation of Σ_{REE} and Eu/Eu* values (Znamenskiy et al., 2014), weak REE fractionation (Monecke et al., 2002), and high Co/Ni (Kun et al., 2014).

Fluid inclusions

Early metamorphogenic pyrite-pyrrhotite mineralization: Fluid inclusion studies suggest similar PTX parameters to regional metamorphism. The gas phase, defined using mass-spectrometry in quartz, arsenopyrite, pyrrhotite, pyrite, and gold (Sazonov et al., unpub. data), is dominated by CO_2, with smaller amounts (up to 10%) of N_2 and CH_4, which is again similar to metamorphogenic fluids at the other gold deposits of Yenisei Ridge.

Gold-arsenic ore studies: Studies show that gold-arsenic ore, represented by disseminated auriferous needle arsenopyrite in association with pyrrhotite-2 and native gold, formed at 335° to 275°C and 1.83- to 0.93-kbars fluid pressure. The mineralizing fluids consist of moderately concentrated (10.4–15.7 wt % NaCl equiv) chloride-carbonate solutions. The gas phase is dominated by N_2 and CH_4, with low concentrations of heavy hydrocarbons, pointing to low redox potential, whereas an absence of CO_2 points to alkaline (pH >7) fluids. This fluid was responsible for the needle (elongate) arsenopyrite, deposited together with gold.

Gold-polymetallic association studies: Isometric arsenopyrite and coarse gold, often with Bi, Pb, and Hg tellurides formed at up to 405°C and 1.76 kbars. The mineralizing fluids were in a heterogeneous state, with gas (CO_2, N_2, and CH_4, 10–13% heavy hydrocarbons) and near-neutral (pH ≤7), low- to moderate-salinity (4.2–11.2 wt % NaCl equiv) phases. This fluid defined the isometric habit of arsenopyrite, which was deposited separately from gold. Consequently, the isometric arsenopyrite reveals low gold grades.

Gold-antimony ore studies: Studies showed that ore formed at 280° to 140°C and <1 kbar from a two-phase fluid. Its gas phase contained CO_2, N_2, and CH_4, varying from predominantly carbonic-acidic to methane-nitrogen-carbonic, with heavy hydrocarbons totalling near 6%. This fluid also contains CO, CS_2, and N-bearing hydrocarbons. The solutions were weakly acidic or near-neutral (pH <7), with bimodal salinities of 4.2 to 11.2 and 22 to 43 wt % NaCl equiv. The latter also contains up to 34 wt % Mn. Low-temperature and weakly acidic to near-neutral fluids explain the absence of arsenopyrite and its low gold grade.

Discussion of the genetic model

Geologic, isotopic, geochronologic, fluid inclusion, and mineralogic studies suggest a long, complex and multistage formation of the Olympiada deposit, with contributions of mantle- and crust-derived fluids, as follows:

1. Localization of mineralization in carbonate-clastic sedimentary rocks, enriched in Au, Ag, As, Sb, and other elements, suggests that they might be both a potential source of metals and an important geochemical trap for gold-sulfide deposition. The Khomolkho Formation might have played a similar role in the formation of the large Sukhoi Log gold deposit in the Bodaibo area in the south of the Siberian craton (Large et al., 2007).
2. Folding and multistage shearing defined the morphology and localization of mineralization.
3. Geochronologic data support long (>150 m.y.) multistage formation of gold mineralization at Olympiada, with the main mineralization introduced at 811 to 750 Ma. However, the possibility cannot be excluded that this wide range of ages reflects resetting of K-Ar, $^{40}Ar/^{39}Ar$, and Rb-Sr ages during multiple metamorphic and magmatic events that may have overprinted mineralization. The long "duration" of mineralization could then simply reflect the duration of these multiple overprinting thermal events.
4. The main stage of mantle and mantle-crustal magmatism of the Yenisei Ridge correlates with the ages of Cu-Ni-Pt (Kingash, Upper Kingash, and Yoko-Dovyren; Polyakov et al., 2013) and REE-carbonatite mineralization (Tomtor) in the Siberian craton, suggesting that the deposit might have formed at a time of extensive mantle-derived magmatism. This magmatism is also synchronous with the Franklin large igneous province (LIP) in North America (Ernst et al., 2016).
5. The 720 to 650 Ma mafic, alkaline mafic, and granitoid magmatism, possibly LIP and rift related, are broadly coeval with the interpreted age of late-stage Au-Sb mineralization. Such rift-related magmatism may have regenerated the system, contributing antimony mineralization.
6. Au-As and Au-Sb mineralization was formed in three main stages by three main types of fluids: (1) moderately concentrated (up to 10–12 wt %) chloride-carbonate solutions with a variable gas phase (CO_2, CH_4, N_2, ±hydrocarbons);

(2) predominantly reduced gas (CH_4, N_2, $H_2O \pm CO_2$, and hydrocarbons); and (3) hypothetical magmatic-related, oxidized fluids of sulfate-carbonate-chloride composition with CO_2-$N_2 \pm H_2S$ gas phase, supposedly related to alkaline mafic melts.

7. Fluid inclusion studies suggest that magmatic-related fluids (type 3 above) might have been responsible for extraction of metals (Au, As, Sb, Hg, Te, Ni, Co) from carbonaceous rocks. Types 1 and 2 fluids were responsible for deposition of economic gold mineralization at Olympiada.
8. Decrease in temperature and changes in pH and redox potential were the most important physicochemical factors in the migration and deposition of Au, As, Sb, and other elements.
9. Some of the above-mentioned characteristics of Olympiada, such as host rocks, close correlation between gold and arsenic, presence of metallic mercury and mercury minerals, submicroscopic size of gold and its occurrence in sulfides, are similar to those of Carlin-type gold deposits (Cline et al., 2005).

Conclusions

Long-term (>150 m.y.) evolution of the multistage mantle-crustal system with multiple sources of mineralization and fluids were responsible for the genesis of the unique Olympiada gold deposit, which shares some characteristics with Carlin-type deposits. Structural and lithologic controls were pivotal in localization of the gold mineralization. The proven vertical extent of mineralization exceeds 1,400 m, and it remains open downdip. It contains >1,564 t Au, grading 4 to 4.6 g/t Au. This could be supplemented by the deep discoveries made in early 2018. The auriferous oxidized ore, developed to a depth of 400 m, contained ca. 200 t of nonrefractory gold, grading 11.1 g/t. In addition, the ores contain economic concentrations of silver and antimony (Olympiada East), as well as tungsten (in oxidized ore).

Acknowledgments

We are grateful to R.G. Sharipov, M.N. Fominykh, and A.L. Popov from Polyus Gold for access to mineral and rock collections as well as for detailed information on historic gold production. A.M. Likhman, A.V. Pridannikov, and A.N. Logachev helped with graphic data. We acknowledge the important contributions to the understanding and development of the deposit by Yu.M. Stragis, who directed the geologic department of Polyus Gold during early mining, and A.A. Plekhanov, S.I. Savushkina, and other geologists. We extend our appreciation to the achievements of Khazret Sovmen, founder and first managing director of Polyus.

A.I. Averchenkov and V.P. Bordonosov, the geologists of the Severnaya Expedition, initiated exploration in the 1960s. A.Y. Kurilin, together with L.V. Li, G.P. Kruglov, and N.F. Gavrilov, discovered Olympiada, whereas V.A. Lopatin, V.I. Arefieva, V.A. Nevolin, and other geologists of Krasnoyarskgeologia identified the main geologic controls during the early years.

The group of A.S. Borisenko from the Institute for Geology and Mineralogy, Siberian Branch, Russian Academy of Sciences in Novosibirsk, contributed to the understanding of mineralization and setting of the deposit.

REFERENCES

Bernatonis, P.B., 1999, Oxidation zone at the Olympiada disseminated gold-sulfide deposit: Abstract of Candidate of Science Dissertation, Tomsk, Tomsk Polytechnic University, 19 p. (in Russian).

Borisenko, A.S., Sazonov, A.M., Nevolko, P.A., Naumov, E.A., Tessalina, S., Kovalev, K.R., and Sukhorukov, V.P., 2014, Gold deposits of the Yenisei Ridge (Russia) and age of its formation [abs.]: Acta Geologica Sinica (English ed.), v. 88 (supp. 2), p. 686–687.

Buryak, V.A., 1982, Metamorphogenic ore mineralization: Nedra, Moscow, 256 p. (in Russian).

Cline, J.S., Hofstra, A.H., Muntean, J.L., Tosdal, R.M., and Hickey, K.A., 2005, Carlin-type gold deposits in Nevada: Critical geologic characteristics and viable models: Economic Geology 100th Anniversary Volume, p. 451–484.

Dobretsov, N.L., 1977, Metamorphism of Mesozoic and Cenozoic fold belts, in Sobolev, V.S., Lepezin, G.G., and Dobretsov, N.L., eds., Metamorphic complexes of Asia: Novosibirsk, Nauka, p. 211–221 (in Russian).

Ernst, R.E., Hamilton, M.A., Soderlund, U., Hanes, J.A., Gladkochub, D.P., Okrugin, A.V., Kolotilina, T., Mekhonoshin, A.S., Bleeker, W., LeCheminant, A.N., Buchan, K.L., Chamberlain, K.R., and Didenko, A.N., 2016, Long-lived connection between southern Siberia and northern Laurentia in the Proterozoic: Nature Geoscience, v. 9, p. 464–469.

Genkin, A.D., 1998, Auriferous arsenopyrite from gold deposits: Inner structure of the grains, composition, mechanisms of growth and forms of gold: Geologia Rudnykh Mestorozhdeniy, v. 40, p. 551–557 (in Russian).

Genkin, A.D., Wagner, F., Krylova, T.L., and Tsepin, A.I., 2002, Auriferous arsenopyrite and conditions of its formation at the Olympiada and Veduga gold deposits (Yenisei Ridge, Siberia): Geologia Rudnykh Mestorozhdeniy, v. 44, p. 59–76 (in Russian).

Gibsher, N.A., Tomilenko, A.A., Sazonov, A.M., Bulbak, T.A. Ryabukha, M.A., Nekrasova, N.A., Khomenko, M.O., and Shaparenko, E.O., 2019, Olympiada gold deposit (Yenisei Ridge): Temperature, pressure, composition of ore-forming fluids, $\delta^{34}S$ of sulfides, $^3He/^4He$ of fluids, Ar-Ar age and continuity of formation: Russian Geology and Geophysics, v. 60, no. 9, p. 1043–1059.

Grigorov, V.T., 2003, The largest gold deposits of the Yenisei Ridge and Kuznetsk Alatau and their economic assessment from the point of view of stratiform mineralization: Moscow, Nauchnyi Mir, 168 p. (in Russian).

Holdaway, M.J., 2000, Application of new experimental and garnet Margules data to the garnet-biotite geothermometer: American Mineralogist, v. 85, p. 881–892.

Henry, D., Guidotti, C., and Thomson, J., 2005, The Ti-saturation surface for low-to-medium pressure metapelitic biotites: Implications for geothermometry and Ti-substitution mechanism: American Mineralogist, v. 90, p. 316–328.

Konstantinov, M.M., Cherkasov, S.V., and Dankovtsov, R.F., 1999, Specific crustal features for large and superlarge endogenic gold deposits (Siberia and Far East regions): Geology Tectonics and Metallogeny, v. 7, p. 143–147 (in Russian).

Korobeinikov, A.F., Ananiev, Y.S., Gusev, A.I., Voroshilov, V.G., Nomokonova, G.G., Pshenichkin, A.Y., and Timkin, T.V., 2013, Ore-metasomatic system and geochemical zonation of goldfields and deposits in the fold belts of Siberia: Tomsk, Tomsk Polytechnic University, 458 p. (in Russian).

Kretschmar, U., and Scott, S.D., 1976, Phase relations involving arsenopyrite in the system Fe–As–S and their application: Canadian Mineralogist, v. 14, p. 364–386.

Kryazhev, S.G., 2017, Genetic models and forecast criteria for gold deposits in the carbonaceous-clastic formations: Doctor of Science Dissertation, Moscow, Central Research Institute of Geological Prospecting for Base and Precious Metals (TSNIGRI), 288 p. (in Russian).

Kun, L., Ruidong, Y., Wenyong, C., Rui, L., and Ping, T., 2014, Trace element and REE geochemistry of the Zhewang gold deposit, southeastern Guizhou Province, China: Chinese Journal of Geochemistry, v. 33, p. 109–118.

Lambert, J.M., Simkovich, G., and Walker, P.L., Jr., 1998, The kinetics and mechanism of the pyrite-to-pyrrhotite transformation: Metallurgical and Materials Transformations, v. 29B, p. 385–396.

Large, R.R., Maslennikov, V.V., Robert, F., Danyushevsky, L.V., and Chang, Z., 2007, Multistage sedimentary and metamorphic origin of pyrite and gold in the giant Sukhoi Log deposit, Lena gold province, Russia: Economic Geology, v. 102, p. 1233–1267.

Li, L.V., 2003, The Olympiada disseminated gold-sulfide deposit: Krasnoyarsk, KNIIGiMS, 120 p. (in Russian).

Likhanov, I.I., and Reverdatto, V.V., 2014, P-T-t constraints on the metamorphic evolution of the Transangarian Yenisei Ridge: Geodynamic

and petrological implications: Russian Geology and Geophysics, v. 55 (3), p. 385–416.
Likhanov, I.I., Polyansky, O.P., Reverdatto, V.V., and Memmi, I., 2004, Evidence from Fe- and Al-rich metapelites for thrust loading in the Transangarian region of the Yenisey Ridge, eastern Siberia: Journal of Metamorphic Geology, v. 22, p. 743–762.
Likhanov, I.I., Reverdatto, V.V., Sukhorukov, V.P., Kozlov, P.S., and Khiller, V.V., 2013, Three metamorphic events in the Precambrian P-T-t history of the Transangarian Yenisey Ridge recorded in garnet grains in metapelites: Petrology, v. 21, p. 561–578.
Likhanov, I.I., Nozhkin, A.D., Reverdatto, V.V., and Kozlov, P.S., 2014, Grenvillian tectonic events and evolution of the Yenisei Ridge at the western margin of the Siberian craton: Geotektonics, v. 48 (5), p. 371–389.
Metelkin, D.V., Vernikovskiy, V.A., and Kazanskiy, A.Y., 2007, Neoproterozoic evolution of Rodinia in the light of new paleomagnetic data at the western margin of the Siberian craton: Russian Geology and Geophysics, v. 48, p. 32–54.
Mkrtychian, A.K., 2007, The source of gold and general characteristics in distribution of gold deposits in the Yenisei Ridge in Mkrtychian, A.K., ed., Geology and mineral resources of central Siberia and adjacent areas: Krasnoyarsk, Krasnoyarskgeols'emka Publishing, p. 52–56 (in Russian).
Monecke, T., Kempe, U., Monecke, J., Sals, M., and Wolf, D., 2002, Tetrad effect in rare earth element distribution patterns: A method of quantification with application to rock and mineral samples from granite-related rare metal deposits: Geochimica et Cosmochimica Acta, v. 66, p. 1185–1196.
Naumov, E.A., Borisenko, A.S., Nevolko, P.A., and Kovalev, K.R., 2015, Gold-sulfide (Au-As) deposits of the Yenisei Ridge (Russia): Age, sources of metals and nature of fluids: Mineral Resources in a Sustainable World: Biennial Society for Geology Applied to Mineral Deposits (SGA) Meeting, 13th, Nancy, 2015, Proceedings, v. 1, p. 165–168.
Novozhilov, Y.I., and Gavrilov, A.M., 1999, Gold-sulfide deposits in carbonaceous-clastic formations: Moscow, TsNIGRI, 175 p. (in Russian).
Novozhilov, Y.I., Gavrilov, A.M., Yablokova, S.V., and Arefieva, V.I., 2014, Unique economic Olympiada gold-sulfide deposit in the upper Proterozoic clastic formations: Rudy i Metally, no. 3, p. 51–64 (in Russian).
Nozhkin, A.D., Turkina, O.M., Maslov, A.V., Dmitrieva, N.V., Kovach, V.P., and Ronkin, Y.L., 2008, Sm-Nd isotopic systematics of Precambrian metapelites from the Yenisei Ridge and variation of the ages in the source of denudation: Doklady Earth Science, v. 423A, no. 9, p. 1495–1500.
Nozhkin, A.D., Borisenko, A.S., and Nevolko, P.A., 2011, Stages of the Late Proterozoic magmatism and ages of gold mineralization in the Yenisei Ridge: Russian Geology and Geophysics, v. 52, p. 158–181.
Petrov, V.G., 1974, Gold metallogeny of the northern Yenisei Ridge: Novosibirsk, Nauka, 140 p. (in Russian).
Polyakov, G.V., Tolstykh, N.D., Mekhonoshin, A.S., Izokh, A.E., Podlipskiy, M.Y., Orsoev, D.A., and Kolotilina, T.B., 2013, Ultramafic-mafic igneous complexes of the Precambrian East Siberian metallogenic province (southern framing of the Siberian craton): Age, composition, origin, and ore potential: Russian Geology and Geophysics, v. 54, p. 1319–1331.
Savichev, A.A., Shevchenko, S.S., Rozinov, M.I., et al., 2006, Isotopic and petrogeochemical characteristics of the Olympiada gold-sulfide deposit and its satellites (Yenisei Range): Regional Geology and Metallogeny, v. 28, p. 122–143.
Sazonov, A.M., 1998, Geochemistry of gold in metamorphic formations: Tomsk, Tomsk Polytechnical University Publishing, 166 p. (in Russian).
Sazonov, A.M., Ananyev, A.A., Poleva, T.V., Khokhlov, A.N., Vlasov, V.S., Zvyagina, E.A., Fedorova, A.V., Tishin, P.A., and Leontyev, S.I., 2010, Gold-ore metallogeny of the Yenisey Ridge: Geological-structural provincialism, structural types of ore fields: Journal of Siberian Federal University, Engineering and Technologies, v. 4, p. 371–395 (in Russian).
Sazonov, A.M., Nekrasova, N.A., Zvyagina, E.A., and Tishin, P.A., 2016, Geochronology of granites, host schists and ores of the Panimba deposit (Yenisei Ridge): Journal of Siberian Federal University, Engineering and Technologies, v. 9 (2), p. 174–188 (in Russian).
Scott, S.D., 1983, Chemical behaviour of sphalerite and arsenopyrite in hydrothermal and metamorphic environments: Mineralogical Magazine, v. 47, p. 427–435.
Serdyuk, S.S., Komorovskiy, Yu.E., Zverev, A.I., Oyaber`, V.K., Vlasov, V.S., Babushkin, V.E., Kirilenko, V.A., and Zemlyanskiy, S.A., 2010, Models of gold deposits in the Yenisei area of Siberia: Krasnoyarsk, Institute Gornogo Dela, Geologii i Geotekhnologiy, 582 p. (in Russian).
Shenfil', V.Yu., 1991, The Late Cambrian of the Siberian platform: Novosibirsk, Nauka, 185 p. (in Russian).
Sovmen, V.K., Stragis, Y.M., Plekhanov, A.A., Bibik, S.M., Krovyakova, L.P., Savushkina, S.I., Lokhmakov, V.A., Zvezdin, I.G., and Logachev, V.S., 2009, Geological structure of gold deposits and experience of geological work at Polyus Company in the Krasnoyarsk region: Krasnoyarsk, Verso, 208 p. (in Russian).
Storozhenko, A.A., Vasiliev, N.F., and Diner, A.E., 2002, Explanatory note to the state geological map of the Russian Federation at a scale of 1:200 000, 2nd ed., Yenisei Series, Sheet O-46-III: Moscow, VSEGEI (in Russian).
Toulmin, P., and Barton, P.B., 1964, A thermodynamic study of pyrite and pyrrhotite: Geochimica et Cosmochimica Acta, v. 288, p. 641–671.
Vernikovskaya, A.E., Metelkin, D.V., et al., 2016, Neoproterozoic structure of the Yenisei Ridge and formation of the western margin of the Siberian craton constrained by geological, paleomagnetic and geochronological data: Geologia i Geofizika, v. 57, p. 63–90 (in Russian).
Vernikovskaya, A.E., Vernikovsky, V.A., Salnikova, E.B., Kotov, A.B., Kovach, V.P., Travin, A.V., and Wingate, M.T.D., 2007, Leucocratic A-type magmatism in evolution of the continental crust at the western margin of the Siberian craton: Russian Geology and Geophysics, v. 48, p. 3–16.
Vernikovsky, V.A., and Vernikovskaya, A.E., 2006, Tectonics and evolution of the granitoid magmatism in the Yenisei Ridge: Russian Geology and Geophysics, v. 47, p. 35–52.
Vernikovsky, V.A., Vernikovskaya, A.E., Kotov, A.B., Salnikova, E.B., and Kovach, V.P., 2003, Neoproterozoic accretionary and collisional events on the western margin of the Siberian craton: New geological and geochronological evidence from the Yenisey Ridge: Tectonophysics, v. 375, p. 147–168.
Vernikovsky, V.A., Metelkin, D.V., Vernikovskaya, A.E., Matushkin, N.Yu., Kazanskiy, A.Yu., Kadilnikov, P.I., Romanova, I.V., Wingate, M.T.D., Larionov, A.N., and Rodionov, N.V., 2016, Neoproterozoic tectonic structure of the Yenisei ridge and formation of the western margin of the Siberian craton based on new geological, paleomagnetic, and geochronological data: Russian Geology and Geophysics, v. 57 (1), p. 63–90.
Volkov, A.V., Sidorov, A.A., Savva, N.E., Prokofiev, V.Y., Kolova, E.E., Savchuk, Y.S., Murashov, K.Y., Sidorova, N.V., Zemskova, M.I., Aristov, V.V., and Wolfson, A.A., 2016, Gold-quartz deposits of the Yana-Kolyma fold belt: Geochemical characteristics of ores and fluids, formation settings: Vestnik SVNTs DVO RAN, no. 3, p. 3–21 (in Russian).
Volobuev, M.I., Stupnikova, N.I., and Zykov, S.I., 1973, Yenisei Ridge, in Polovinkin, Yu.I., ed., Geochronology of the USSR, v. 1, Precambrian: Leningrad, Nedra, p. 189–201 (in Russian).
Vrublevskiy, V.V., Nikitin, R.N., Tishin, P.A., and Travin, A.V., 2017, Metamafic rocks of the Middle Transangara region, Yenisei Ridge: E-MORB relics of Neoproterozoic lithosphere: Litosfera, v. 17 (5), p. 67–84 (in Russian).
Winkler, H.G.F., 1979, Petrogenesis of metamorphic rocks: New York, Springer, 339 p.
Wu, C.-M., Zhang, J., and Ren, L., 2004, Empirical garnet-biotite-plagioclase-quartz (GBPQ) geobarometry in medium- to high-grade metapelites: Journal of Petrology, v. 45, p. 1907–1921.
Yakubchuk, A., Stein, H., and Wilde, A., 2014, Results of pilot Re-Os dating of sulfides from the Sukhoi Log and Olympiada orogenic gold deposits, Russia: Ore Geology Reviews, v. 59, p. 21–28.
Zabiyaka, A.I., Kurgankov, P.P., Gusarov, Yu.V., et al., 2004, Tectonics and metallogeny of the Lower Angara region: Krasnoyarsk, KNIIGiMS, 322 p. (in Russian).
Znamenskiy, S.E., Michurin, S.V., Velivetskaya, T.A., and Znamenskaya, N.M., 2014, Structural setting and possible sources of mineralization in the Ganeevskoe gold deposit (South Urals): Litosfera, no. 6, p. 118–131 (in Russian).
Zuev, V.K., Kachevskiy, L.K., Kachevskaya, G.I., Komarov, V.V., Minaeva, O.A., Markovich, L.A., Shatalina, T.N., and Potapenko, L.Y., 2009, Explanatory note to the state geological map of the Russian Federation at a scale of 1:1000000 (3rd generation): Angara-Yenisei Series, Sheet O-46 Krasnoyarsk: St.-Petersburg, VSEGEI, 500 p.
Zvyagina, E.A., 1989, Metamorphism and gold metallogeny of the Upper Enashimo ore cluster: Candidate of Science Dissertation, Krasnoyarsk, Siberian Federal University, 275 p. (in Russian).